Journal of Physiology (1993), **466**, *pp.* 443–480
With 17 figures
Printed in Great Britain

THE MECHANISM OF ION TRANSPORT BY THE Na^+–Ca^{2+}, K^+ EXCHANGE IN RODS ISOLATED FROM THE SALAMANDER RETINA

BY R. J. PERRY* AND P. A. MCNAUGHTON†

From the Physiology Department, King's College London, Strand, London WC2R 2LS and the Physiological Laboratory, University of Cambridge, Cambridge CB2 3EG

(*Received 4 September 1992*)

SUMMARY

1. Membrane currents caused by the operation of electrogenic Na^+–Ca^{2+}, K^+ exchange were recorded from isolated rod outer segments under voltage-clamp using a whole-cell electrode.

2. Reversed mode exchange currents (Na_i^+–Ca_o^{2+}, K_o^+) were recorded with a high internal [Na^+] and when both Ca^{2+} and K^+ were present in the external solution. Omission of either Ca^{2+} or K^+ completely suppressed both the reversed exchange current and the entry of Ca^{2+}.

3. The charge transferred by the exchange per Ca^{2+} ion transported was identical in both forward and reversed modes.

4. The reversed exchange current declined as Ca^{2+} accumulated inside the outer segment, and the form of this decline was consistent with a first-order inhibition by internal Ca^{2+}.

5. The reversed exchange current was increased e-fold by a 230 mV depolarization over the range -51 to $+29$ mV.

6. The activation of reversed exchange by external Ca^{2+} was well described by first-order kinetics with a Michaelis constant, $K_{Ca_o}^{app}$, of 34 μM in the presence of 20 mM external K^+. $K_{Ca_o}^{app}$ was reduced by lowering external [K^+], was increased by adding external Na^+ and was unaffected by membrane potential.

7. External K^+ also activated the exchange in a first-order manner with a Michaelis constant, $K_{K_o}^{app}$, of 151 μM in the presence of 0·5 mM external Ca^{2+}. $K_{K_o}^{app}$ was reduced by lowering external [Ca^{2+}], increased by adding external Na^+ and was unaffected by membrane potential.

8. When the level of internal Ca^{2+} was increased via reversed exchange, $K_{Ca_o}^{app}$ diminished in proportion to the reduction in the maximum current, but $K_{K_o}^{app}$ remained approximately constant.

9. These observations cannot be reconciled with simple models of the exchange in which ions bind simultaneously at opposite faces of the membrane before transport occurs. The results are broadly consistent with a consecutive model of the exchange in which unbinding of Na^+ at either the external or the internal membrane surface

* Present address: William Osler House, John Radcliffe Hospital, Oxford OX3 9DU.
† Present address: Physiology Department, King's College, Strand, London WC2R 2LS.

MS 1759

is followed by binding of Ca^{2+} and then K^+, and are fully reproduced by a model in which Ca^{2+} binds before all of the Na^+ has dissociated from the exchange molecule.

INTRODUCTION

It has recently become apparent that the Ca^{2+} transport mechanism in rod outer segments, which had previously been known as Na^+–Ca^{2+} exchange, in fact both requires and transports K^+ ions (Cervetto, Lagnado, Perry, Robinson & McNaughton, 1989; Schnetkamp, Basu & Szerencsei, 1989; Friedel, Wolbring, Wohlfahrt & Cook, 1991; Leser, Nicoll & Applebury, 1991), and should therefore be called the Na^+–Ca^{2+}, K^+ exchange. Using electrophysiological techniques it has been demonstrated that the stoichiometry of the exchange near equilibrium is $4Na^+$ *vs.* $1K^+$ and $1Ca^{2+}$ (Cervetto *et al.* 1989). It has since been suggested that the coupling between Na^+, Ca^{2+} and K^+ is variable, so that the K_o^+ dependence of reversed (Na_i^+–Ca_o^{2+}, K_o^+) exchange is almost zero in the presence of a large inward Ca^{2+} gradient (Schnetkamp, Szerencsei & Basu, 1991). In the present study we have re-addressed the question of the requirement of the exchange for K_o^+, and we find that the K_o^+ dependence is absolute even when the exchange is far from equilibrium.

The ion dependence of the exchange current can be used to elucidate the transport mechanism of the exchange. Hodgkin & Nunn (1987) showed that the apparent Michaelis constant with which Ca_i^{2+} activates forward (Na_o^+–Ca_i^{2+}, K_i^+) exchange is not affected by reducing $[Na^+]_o$ from 110 to 55 mM. This observation led them to adopt a one-step simultaneous model of the exchange, a feature of which was that the ionic concentrations on one side of the outer segment membrane did not influence the apparent affinities with which ions bound on the other side of the membrane.

We have carried out a series of experiments with the aim of testing various models of the transport mechanism. Following on from previous observations that the Na_o^+ dependence of forward exchange is strongly voltage dependent (Lagnado, Cervetto & McNaughton, 1988), we examined the Ca_o^{2+} and K_o^+ dependence of the reversed mode, and found both to be voltage independent. This observation suggests that charge is transferred during the translocation of Na^+ but not during the translocation of Ca^{2+} and K^+.

Reversed exchange currents rapidly decline, and the form of the decline is consistent with the hypothesis that Ca_i^{2+} accumulates and inhibits reversed exchange in a first-order manner. The rise in $[Ca^{2+}]_i$ was found to increase the apparent affinity of the exchange for Ca_o^{2+} without much affecting the apparent affinity of the exchange for K_o^+.

The observations that $[Ca^{2+}]_i$ can influence the Ca_o^{2+} dependence but not the K_o^+ dependence of the exchange, and that Na_o^+ competes with Ca_o^{2+} and K_o^+ for exchange sites, led us to abandon simple simultaneous models and adopt instead a consecutive model, in which the Na^+ and $Ca^{2+} + K^+$ translocation steps are separate events (see Discussion). Our other experimental observations have been used to refine the model, and the properties of the final 'ten-state' model have been compared with experimental observations from the Na^+–Ca^{2+}, K^+ exchange literature. A preliminary report of these experiments has appeared (Perry & McNaughton, 1991).

METHODS

Isolation of rod outer segments

Larval tiger salamanders (*Ambystoma tigrinum*, Lowrance Waterdog Farms, OK, USA) were dark-adapted for at least an hour before experiments and were killed by decapitation followed by pithing. Eyes were rapidly isolated under dim red illumination; all subsequent dissection and experimental procedures were carried out using infrared illumination since it could not be guaranteed that light would not modify the properties of the exchanger. The method for mechanically dissociating single rods from the retina, described by Hodgkin, McNaughton, Nunn & Yau (1984), also yielded detached rod outer segments from which whole-cell recordings could be made (Sather & Detwiler, 1987; Lagnado *et al.* 1988). All experiments were performed at room temperature (18–22 °C).

Recording chamber and optics

The recording chamber was made from Perspex sandwiched between a piece of a glass microscope slide above and a coverslip below, and had a capacity of about 280 μl. To reduce cell adhesion, the coverslip was coated with tri-*n*-butyl chlorosilane (as described for electrodes by Lamb, McNaughton & Yau, 1981). This chamber was mounted on the stage of an inverted compound microscope (Zeiss IM35) connected to a closed-circuit TV system (Panasonic WV1850). The front of the chamber remained open to allow the insertion of electrodes: the solution was retained in the recording chamber by surface tension. The perfusion system was similar to that described by Hodgkin, McNaughton & Nunn (1985, 1987), except that solutions were fed into the rear of the chamber through four parallel slots cut into the Perspex. Solution changes were achieved within 30–100 ms. The electrical potential of the recording chamber was controlled by the feedback system of Hodgkin *et al.* (1984).

Solutions and pipettes

Ringer solution contained 110 mM NaCl, 2·5 mM KCl, 1·0 mM $CaCl_2$, 1·6 mM $MgCl_2$ and, as with all external solutions, 10 mM of the pH buffer *N*-2-hydroxyethylpiperazine-*N'*-2-ethanesulphonic acid (Hepes), neutralized to pH 7·6 with tetramethylammonium hydroxide (TMA-OH). In a typical experimental protocol, outer segments were depleted of Ca^{2+} by fully activating forward mode Na^+–Ca^{2+}, K^+ exchange in a solution containing 114·4 mM NaCl, 0 $CaCl_2$, 0 KCl and 2 mM of the Ca^{2+} and Mg^{2+} chelator, ethylenediaminetetraacetic acid (EDTA). Outer segments were then exposed to a 0 Na^+, 0 Ca^{2+} solution containing $(114{\cdot}4-x)$ mM choline chloride, x mM KCl and 2 mM EDTA, where x is a concentration of KCl between 0 and 20 mM. Reversed exchange was activated by removing the EDTA and adding various concentrations of $CaCl_2$ to this solution. Experiments on the effect of Na_o^+ were performed with various concentrations of Na_o^+ replacing the same choline concentrations in both the 0 Ca^{2+} and the Ca^{2+}-containing solutions. Low-Ca^{2+} solutions were produced using 823 μM $CaCl_2$ + 2 mM *N*-hydroxyethylethylenediaminetriacetic acid (HEDTA) to achieve a free $[Ca^{2+}]$ of 1 μM and 6·8 mM $CaCl_2$ + 0·5 mM nitrilotriacetic acid to achieve a free $[Ca^{2+}]$ of 10 μM Ca^{2+}; higher concentrations of Ca^{2+} were unbuffered. The absence of K^+ from 0 K^+ solutions was confirmed by flame photometry ($[K^+] < 10$ μM).

Suction pipettes used to hold the outer segment in the flowing solution were prepared by the methods of Baylor, Lamb & Yau (1979), 'silanized' by the methods of Lamb, McNaughton & Yau (1981) and filled with a solution containing 116·4 mM LiCl or 116·4 mM choline chloride and 10 mM Hepes neutralized to pH 7·6 with TMA-OH. The absence of Na^+, K^+ and Ca^{2+} from the solution in the suction pipette ensured that no forward or reversed exchange occurred in the small portion of the outer segment membrane which was exposed to this solution. In a few early experiments, Ca^{2+} chelators were included in the suction pipette solution, but these appeared to reduce membrane stability, and were omitted in all of the experiments reported here.

Whole-cell pipettes were pulled from borosilicate glass of external diameter 1·8 mm (100 μl pipettes, Farmitalia Carlo Erba, Italy) on a two-stage horizontal puller (BB-Ch, Mecanex, Geneva) and were held in a Perspex pipette holder containing a Ag–AgCl electrode (Clark Electromedical Instruments). The holder was inserted directly into the headstage of a commercial patch-clamp amplifier (Model 8900, Dagan Instruments, Minneapolis) with a 10 GΩ feedback resistor. The internal diameter of the tip of each pipette was about 0·8 μm, corresponding to a bubble number of 5·4–5·6 in clean methanol (see Corey & Stevens, 1983).

Whole-cell pipettes were filled with a solution containing 110 mM sodium aspartate, 5 mM potassium aspartate, 3 mM $MgCl_2$, 1 mM Na_2ATP and 10 mM Pipes (piperazine-*N*-*N'*-bis(ethanesulphonic acid) neutralized to pH 7·1 using NaOH, giving a final $[Na^+]$ of 129 mM. Na_2GTP and cyclic GMP were omitted from the pipette, and light-sensitive currents were therefore never observed (cf. Lagnado *et al.* 1988). The liquid junction potential between the whole-cell pipette solution and Ringer solution was found to be −11 mV using a method similar to that of Fenwick, Marty & Neher (1982); all membrane potentials have been corrected accordingly.

Isolated rod outer segments were picked up off the floor of the bath and held in the mouth of a suction pipette by gentle suction. The tip of the whole-cell pipette was then brought against the outer segment membrane and suction applied in order to obtain a whole-cell recording with a seal resistance of 10–40 GΩ (Sather & Detwiler, 1987; Lagnado *et al.* 1988).

Data acquisition and analysis

All data were stored on analog tape (Store 7DS, Racal Recorders, Hythe). Traces were digitized, on-line or from tape, on a PDP 11-73 minicomputer (Plessey Peripheral Systems, Surbiton), using a CED 502 interface (Cambridge Electronic Design, Cambridge), filtering at half the sampling frequency using an eight-pole Butterworth filter (Kemo, Kent). No further filtering of the traces was required. Ion dependence data were fitted to Michaelis functions using a commercial non-linear regression program (Enzfitter, Elsevier Biosoft, Cambridge).

RESULTS

Absolute requirement of reversed Na^+–Ca^{2+}, K^+ exchange for K_o^+

We have previously shown that little or no reversed exchange current can be elicited from the rod outer segment in the absence of K_o^+ (Cervetto *et al.* 1989). This observation implies that the reversed mode of the exchange is dependent on K_o^+, but exchange currents measured even in the presence of K_o^+ were quite small in those experiments because the exchange was close to equilibrium. Figure 1 shows an experiment in which the exchange was far from equilibrium, and provides a more stringent test of the requirement of reversed exchange for K_o^+. This experiment, in common with all of the experiments described in this paper, was performed with a whole-cell pipette solution containing 129 mM Na^+, 5 mM K^+ and zero added Ca^{2+} (see Methods for other constituents). Before the start of each trace in Fig. 1, the outer segment was depleted of Ca_i^{2+} by fully activating forward exchange in an external solution containing 114·4 mM Na^+ but no K^+ or Ca^{2+}. The forward exchange current was allowed to decline to zero, indicating that the free $[Ca^{2+}]_i$ had been reduced to a very low level, and Na_o^+ was then replaced with choline. In traces 2 and 4, 0·5 mM Ca_o^{2+} and 20 mM K_o^+ were then both added. As would be expected, given that there was now a large outward Na^+ gradient and inward gradients for both Ca^{2+} and K^+, a large outward exchange current was activated. This current was immediately suppressed when Ca_o^{2+} and K_o^+ were removed, and the return of the current to its initial value shows that there was no change in the baseline. Subsequent exposure to the solution containing 114·4 mM Na^+, 0 Ca^{2+} activated a transient inward exchange current as the Ca^{2+} load was pumped back out of the outer segment, confirming that the outward current in the test solution had indeed been associated with an influx of Ca^{2+}. Note that the inward current in the presence of 114·4 mM Na_o^+ finally declined to a steady level 16 pA below that observed in the 0 Na^+ solutions at the start; the difference is attributable to a junction current caused by the liquid junction potential between the 0 Na^+ and Na^+-containing solutions.

Traces 1 and 3 of Fig. 1 show similar solution changes, but with only 0·5 mM Ca^{2+}

(trace 1) or only 20 mM K^+ (trace 3) in the test solution. The experiment shows that neither of these cations alone is capable of activating a reversed exchange current. No change in current was seen on addition of 0·5 mM Ca_o^{2+}, while adding 20 mM K_o^+ elicited a small inward shift in baseline attributable to a junction current between the K^+- and choline-containing solutions.

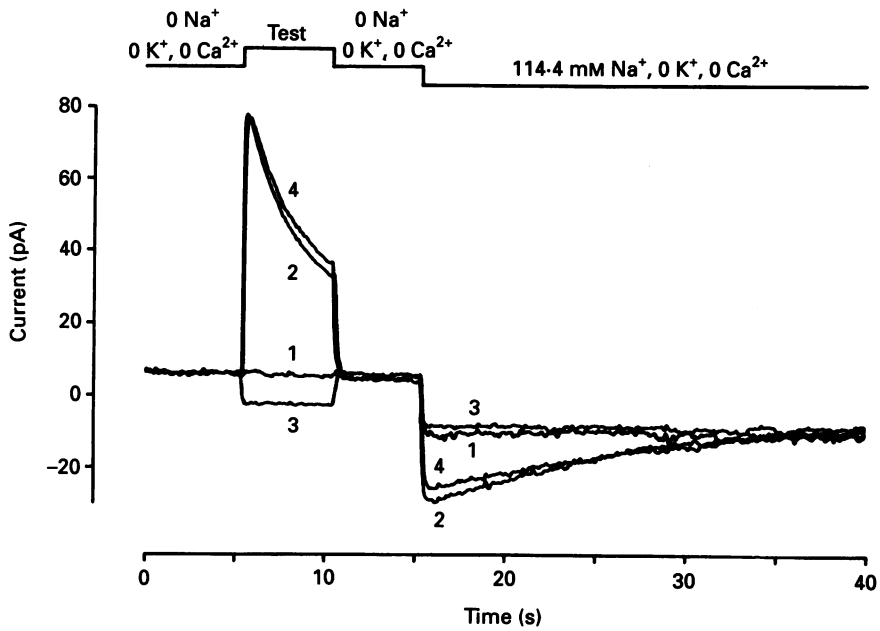

Fig. 1. Currents activated on addition of Ca_o^{2+} alone, K_o^+ alone or Ca_o^{2+} and K_o^+ together. Before start of trace, $[Ca^{2+}]_i$ was reduced to zero in a solution containing 114·4 mM Na_o^+, 0 K_o^+ and 0 Ca_o^{2+} (+2 mM EDTA), and then Na_o^+ replaced by choline to give '0 Na^+, 0 K^+, 0 Ca^{2+}' solution in which choline is the only external cation. At time = 5 s, 0·5 mM Ca_o^{2+} (trace 1), 20 mM K_o^+ (trace 3) or 0·5 mM Ca_o^{2+} + 20 mM K_o^+ (traces 2 and 4) was added. Note that outward (reversed) exchange current is activated only when both Ca_o^{2+} and K_o^+ are added together. On readmission of 114·4 mM Na_o^+, traces 1 and 3 show inward shift caused by a change in the junction current as a result of the liquid junction potential between 0 Na^+ and Na^+-containing solutions. Traces 2 and 4 show a transient inward exchange current superimposed on this shift. Holding potential, −11 mV.

One explanation for the absence of a reversed exchange current when Ca_o^{2+} alone is added to the external solution (trace 1 in Fig. 1) could be that, in the absence of K_o^+, reversed exchange is forced to operate in an electroneutral mode such as $2Na^+$ *vs.* $1Ca^{2+}$. This possibility is eliminated by the observation that, when 114·4 mM Na_o^+ was restored, no forward exchange current was observed. This observation demonstrates that no Ca^{2+} entered the outer segment during the exposure to 0·5 mM Ca_o^{2+}, 0 K_o^+. There is therefore no K^+-independent route for Ca^{2+} entry, either via the exchange or via other mechanisms.

In some experiments a small outward exchange current was seen during the exposure to the 0·5 mM Ca_o^{2+}, 0 K_o^+ solution, and in seven outer segments the mean exchange current activated by the 0·5 mM Ca_o^{2+}, 0 K_o^+ solution, expressed as a

proportion of the exchange current activated by 0·5 mM Ca_o^{2+}, 20 mM K_o^+, was 4·8%. The standard deviation of this proportion was 2·1%, indicating that the value was very variable, but it was always less than 7%. It is possible that this small current represents K_o^+-insensitive reversed exchange, but in view of the high affinity of the exchange for K_o^+ (see below), it seems more likely that the current represents activation of the exchange by residual traces of K^+, since a contamination level of only 15 μM $[K^+]_o$ would be sufficient to activate 10% of the reversed exchange current. Considerable rinsing of the solution pipes with the 0 K^+ solution was required to eliminate traces of the 20 mM K_o^+ which had been used in previous solution changes.

Equality of charge flow through forward and reversed exchange

If the stoichiometry of the exchange is identical in forward and reversed modes then the charge transferred out of the outer segment during the entry of a given Ca^{2+} load via reversed exchange should be equal and opposite to the charge entering the outer segment when the same load is extruded via forward exchange. Figure 2 shows that this is the case. At the start of the trace the Ca^{2+}-depleted outer segment was bathed in a solution containing 20 mM KCl, with 0 Na_o^+ and Ca_o^{2+} preventing the operation of both the forward and the reversed modes of the exchange. Admission of 1 mM $CaCl_2$ activated a large outward exchange current, all of which can be attributed to the operation of reversed exchange since the addition of Ca_o^{2+} itself causes no measurable change in the junction current (see Fig. 1, trace 1). The charge transferred by reversed exchange was obtained from integration of the current trace (Fig. 2*A*, lower panel), using the current in the 20 mM K^+, 0 Na^+ and Ca^{2+} solution (during time interval *r*) as the zero level.

Readmission of Na_o^+ activated a forward exchange current as Ca^{2+} was pumped back out of the outer segment, and integration of this current showed that the charge transferred was equal and opposite to that flowing during reversed exchange. The zero level for integration was taken as the final steady current level in the Na^+-containing solution to allow for the small difference in junction current between the 0 Na^+ and 114·4 mM Na^+ solutions (see Fig. 1). The equality of charge flow per Ca^{2+} ion transported via reversed and forward exchange was also found to hold at much lower $[Ca^{2+}]_o$ levels (e.g. 1·4 μM in Fig. 2*B*). These observations confirm that the charge transferred per Ca^{2+} is the same for both the forward and reversed modes of the exchange (Cervetto *et al.* 1989) and that in the absence of any open light-sensitive channels, the exchange is the only pathway by which Ca^{2+} may cross the outer segment membrane (see also Lagnado & McNaughton, 1991).

Decline of reversed exchange current

Reversed exchange currents such as that activated by 1 mM Ca^{2+} in Fig. 2*A* begin to decline immediately because the Ca^{2+} which is transported into the outer segment by reversed exchange competes with Na_i^+ for exchange sites. If the inhibition of reversed exchange by free Ca_i^{2+} can be described by simple first-order kinetics, then the relationship between the exchange current, *j* and $[Ca^{2+}]_i$ has the form

$$\frac{j}{j_{max}} = \frac{A}{A + [Ca^{2+}]_i}, \quad (1)$$

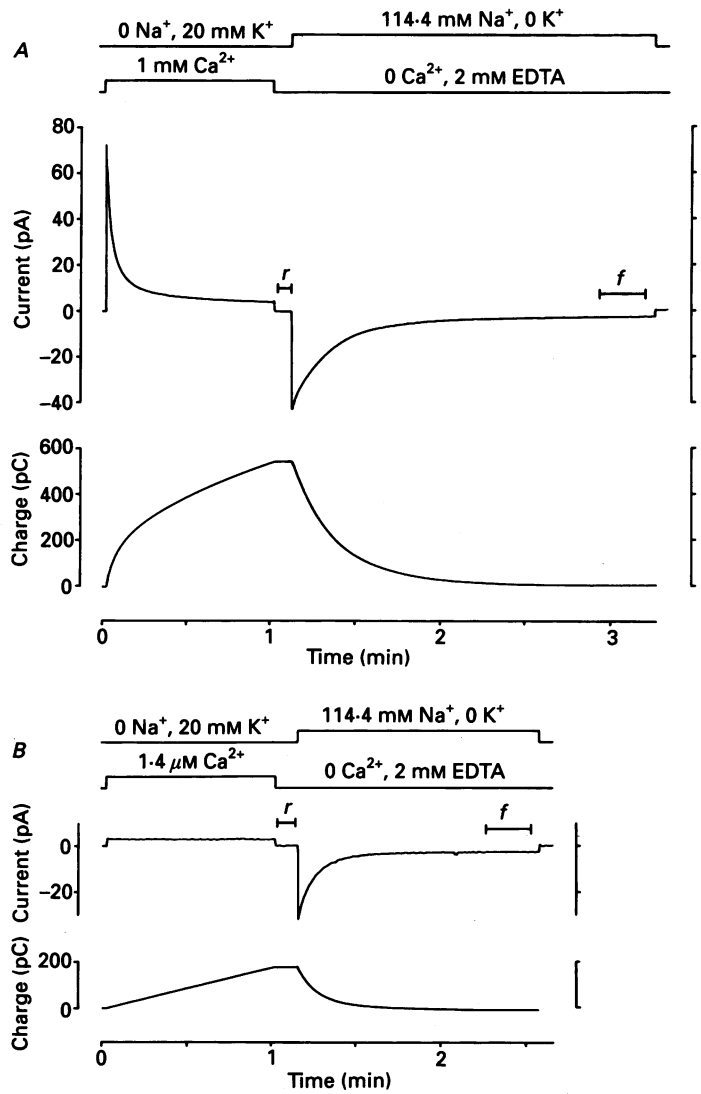

Fig. 2. Equality of charge flow through forward and reversed exchange. Before start of each trace, $[Ca^{2+}]_i$ was reduced to zero in 114·4 mM Na_o^+, 0 K_o^+, 0 Ca_o^{2+}, and outer segment then transferred to 0 Na_o^+, 20 mM K_o^+ and 0 Ca_o^{2+}. All 0 Ca_o^{2+} solutions contained 2 mM EDTA. Holding potential, −11 mV throughout. *A*, upper trace: large reversed (outward) exchange current activated on addition of 1 mM Ca_o^{2+}; trace falls back to zero when Ca_o^{2+} withdrawn again 1 min later. Large transient forward (inward) exchange current activated when K_o^+ removed and 114·4 mM Na_o^+ added (Ca_o^{2+} still zero). Trace returns to zero when Na_o^+ removed and 20 mM K_o^+ restored. *A*, lower trace: integral of exchange currents, to show charge transferred. Reversed exchange current integrated taking as zero level the mean current during time interval *r*. Forward exchange current integrated taking as zero level the mean current during time interval *f*. *B*, as for *A*, but using 1·4 μM Ca_o^{2+} in place of 1 mM Ca_o^{2+}.

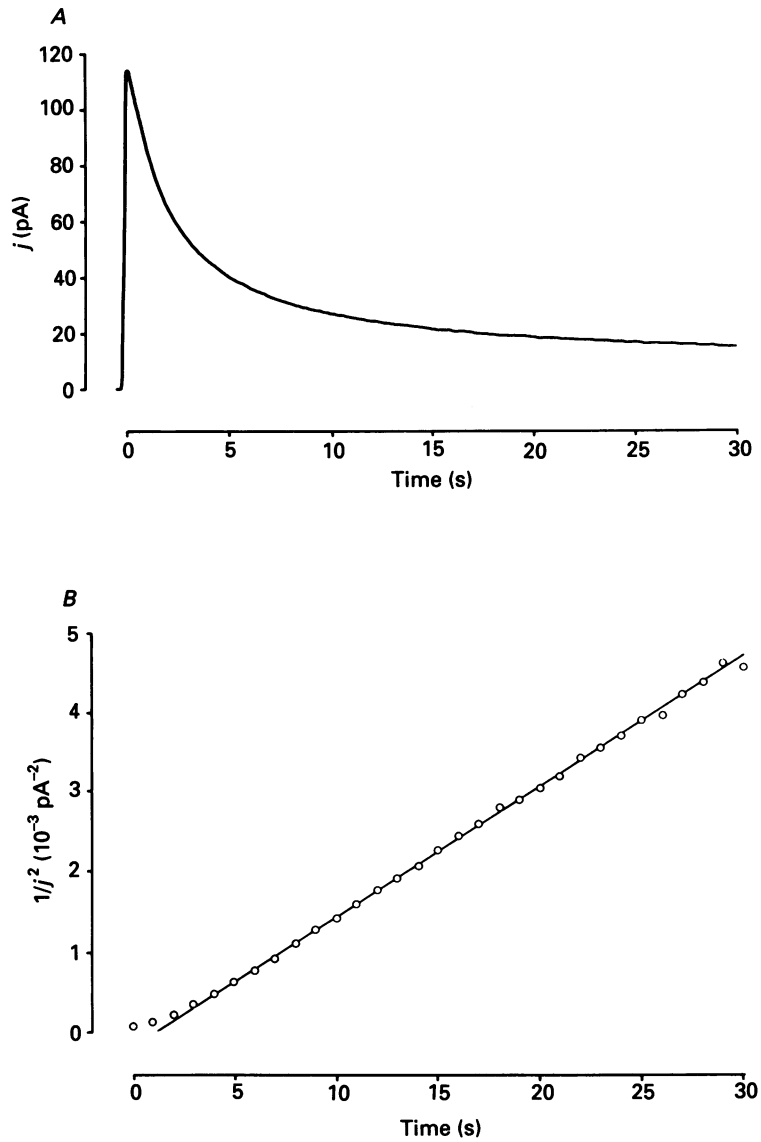

Fig. 3. Form of decline of reversed exchange current. *A*, reversed exchange current, j, activated by the addition of 0·5 mM Ca_o^{2+} to an outer segment with 0 Na_o^+, 20 mM K_o^+ and 0 Ca_i^{2+} present throughout. Holding potential, −11 mV. *B*, circles represent data points from curve shown in *A*, plotted on a scale of $1/j^2$ against time. The continuous line represents a linear regression of the data points between 5 and 30 s on the time axis, and is equivalent to eqn (5) with j_{max} = 114·5 pA, A = 47·6 μM, V = 1·39 pl, B = 15·9, $t(0)$ = 5 s and $j(0)$ = 39·7 pA.

where j_{max} is the value of the exchange current in the absence of Ca_i^{2+} and A is a constant. Differentiating with respect to $[Ca^{2+}]_i$ and inserting eqn (1) gives

$$\frac{dj}{d[Ca^{2+}]_i} = \frac{-j^2}{Aj_{max}}. \quad (2)$$

Given that one net positive charge is transferred in exchange for each Ca^{2+} transported (Yau & Nakatani, 1984; Hodgkin *et al.* 1987; Lagnado & McNaughton, 1991), it will also be true that

$$\frac{d[Ca]_T}{dt} = \frac{j}{FV}, \tag{3}$$

where $[Ca]_T$ is the total (free and bound) [Ca] in the outer segment, F is the Faraday constant and V is the cytosolic volume of the outer segment. Calcium is buffered within the outer segment by two systems: a high-affinity buffer of limited capacity and a low-affinity, large-capacity buffer (Lagnado, Cervetto & McNaughton, 1992). Once enough calcium has entered to saturate the high-affinity buffer, then the relationship between $[Ca]_T$ and $[Ca^{2+}]_i$ is given by the equation:

$$[Ca]_T = C + (B+1)[Ca^{2+}]_i,$$

where B is the ratio of [Ca] bound to the low-affinity buffer to the free $[Ca^{2+}]$, and C is the capacity of the high-affinity buffer (Lagnado *et al.* 1992). Equation (3) may therefore be rewritten as

$$\frac{d[Ca^{2+}]_i}{dt} = \frac{j}{FV(B+1)}. \tag{4}$$

Applying the chain rule to eqns (2) and (4) gives

$$\frac{dj}{dt} = \frac{-j^3}{AFV(B+1)j_{max}}.$$

Integrating with respect to j gives

$$\frac{1}{j^2} = \frac{2}{j_{max}AFV(B+1)}\{t - t(0)\} + \frac{1}{j(0)^2}, \tag{5}$$

where $t(0)$ is the time at which the high-affinity buffer becomes fully saturated with Ca^{2+} and $j(0)$ is the current at this time.

Figure 3*A* shows the reversed exchange current elicited by the addition of 0·5 mM Ca^{2+} in an experiment similar to that shown in Fig. 2*A*. In Fig. 3*B* this current trace has been transformed to give a plot of j^{-2} as a function of time (○). As predicted by eqn (5), once sufficient Ca^{2+} has entered to fully saturate the high-affinity buffer, this function becomes linear. The continuous line in Fig. 3*B* represents eqn (5) with j_{max} = 114·5 pA, A = 47·6 μM, V = 1·39 pl, B = 15·9 (Lagnado *et al.* 1992), $t(0)$ = 5 s and $j(0)$ = 39·7 pA. The form of the decline of the reversed exchange current is therefore consistent with a first-order inhibition of the reversed exchange by Ca_i^{2+}.

Voltage dependence of the reversed exchange current

Lagnado *et al.* (1988) found that the voltage sensitivity of the forward exchange current activated by a saturating $[Ca^{2+}]_i$, when other internal and external ions were close to their physiological concentrations, was described by an exponential relationship with an e-fold reduction in current for a 70 mV depolarization. In the present study, reversed exchange currents were activated by the addition of 0·5 mM Ca^{2+} with 20 mM K^+ throughout (as in Fig. 3*A*), first at the holding potential of

−11 mV, then at various other potentials between −71 and +29 mV, returning to the holding potential again for every second or third reversed exchange current in the series. For each membrane potential the peak amplitude of the reversed exchange current was obtained relative to the amplitude at −11 mV, and the mean relative

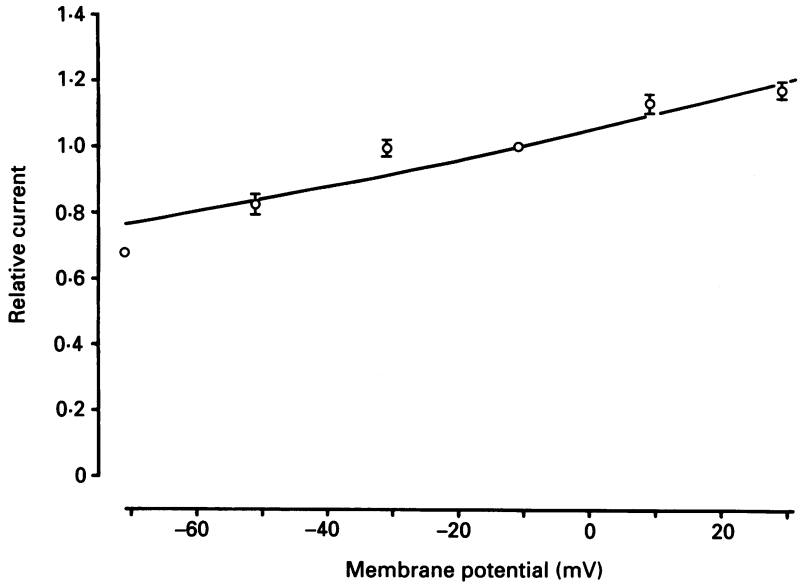

Fig. 4. Voltage dependence of initial exchange current amplitude. Each current measurement was expressed relative to the mean control current measurement made at −11 mV in the same outer segment. Bars represent standard errors of means from three to four outer segments. Point at −71 mV represents a single estimate. Continuous curve given by the expression: relative current = $\exp[(V_m + 11)/230]$ where V_m is the membrane potential (in mV).

currents from seven rod outer segments are plotted in Fig. 4. The best exponential fit to the data, with an e-fold change in current for every 230 mV, is shown by the continuous line. In the ionic conditions of these experiments, therefore, the reversed mode of the exchange is only weakly voltage dependent.

Dependence of reversed exchange on $[Ca^{2+}]_o$

Figure 5*A* illustrates the method used to obtain the dependence of the reversed exchange current on $[Ca^{2+}]_o$. Before each trace the outer segment was depleted of Ca_i^{2+} (see above) and at time zero the concentration of Ca_o^{2+} indicated beside the trace was added, with 20 mM K_o^+ present throughout. As shown in Fig. 5*B*, the dependence of the exchange on $[Ca^{2+}]_o$ in the presence of 0 Na_o^+ and 20 mM K_o^+ was well described by a Michaelis relation with an apparent Michaelis constant, $K_{Ca_o}^{app}$, of 34 ± 1 μM (mean ± S.E.M. from nineteen outer segments). By contrast, the Michaelis constant with which Ca_i^{2+} activates forward exchange in near-physiological conditions is 1·6 μM (Lagnado *et al.* 1992), i.e. the apparent Ca^{2+} affinity is much higher at the internal face. This discrepancy is unlikely to result from differences in the concentrations of competing cations: the lower concentration of K^+ and the absence

of Mg^{2+} on the same side as Ca^{2+} in the present experiments, as compared with the values in the intact rod, would be expected to increase the apparent Ca^{2+} affinity measured at the external face (see below and Hodgkin & Nunn, 1987). The intrinsic Ca^{2+} affinity of the exchange at its external surface must therefore be considerably lower than at the internal surface.

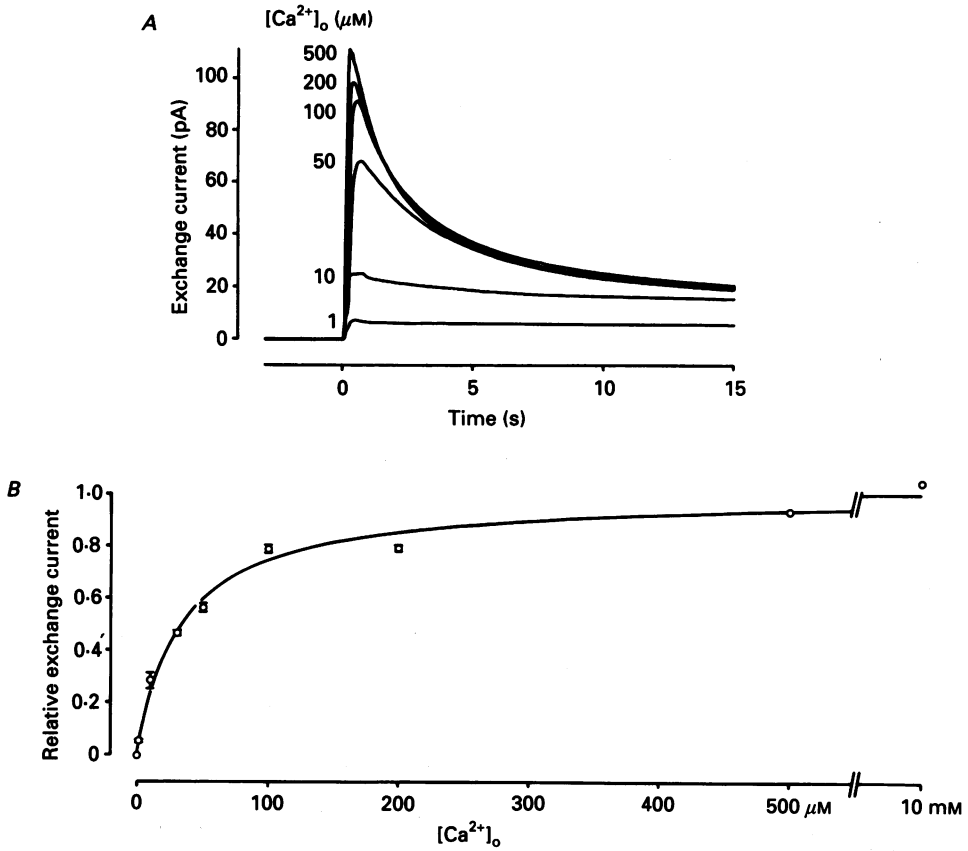

Fig. 5. Ca_o^{2+} dependence of reversed exchange current. *A*, series of exchange currents activated by addition of various concentrations of Ca_o^{2+} with 20 mM K_o^+ present throughout. Traces have been aligned on the current axis so that the zero levels coincide. Holding potential, −11 mV. *B*, curve showing initial amplitude of exchange current as a function of $[Ca^{2+}]_o$. Bars represent standard errors of mean estimates from three to fourteen outer segments. Includes data from a total of nineteen outer segments. Continuous curve represents the Michaelis function: relative current = $[Ca^{2+}]_o/(K_{Ca_o}^{app}+[Ca^{2+}]_o)$. The curve of best fit, found using a least-squares curve-fitting routine (see Methods), gave $K_{Ca_o}^{app} = 34 \pm 1$ μM (mean ± S.E.M.).

Influence of V_m, $[K^+]_o$ and $[Na^+]_o$ on Ca_o^{2+} dependence

The following procedure was used to establish the Ca_o^{2+} dependence of the exchange in a wide range of conditions. In control conditions (membrane potential, V_m = −11 mV, $Na_o^+ = 0$ and $K_o^+ = 20$ mM) reversed exchange currents were activated with a saturating concentration of Ca_o^{2+} (usually 0·5 mM), then with a concentration

which was approximately half-saturating (usually 30 μM), and finally with the saturating concentration once more. Given the first-order Ca_o^{2+} dependence of the exchange (see Fig. 5*B*), an estimate of the $K_{Ca_o}^{app}$ could be obtained from these two points on the Michaelis curve. Similar measurements were then made under test

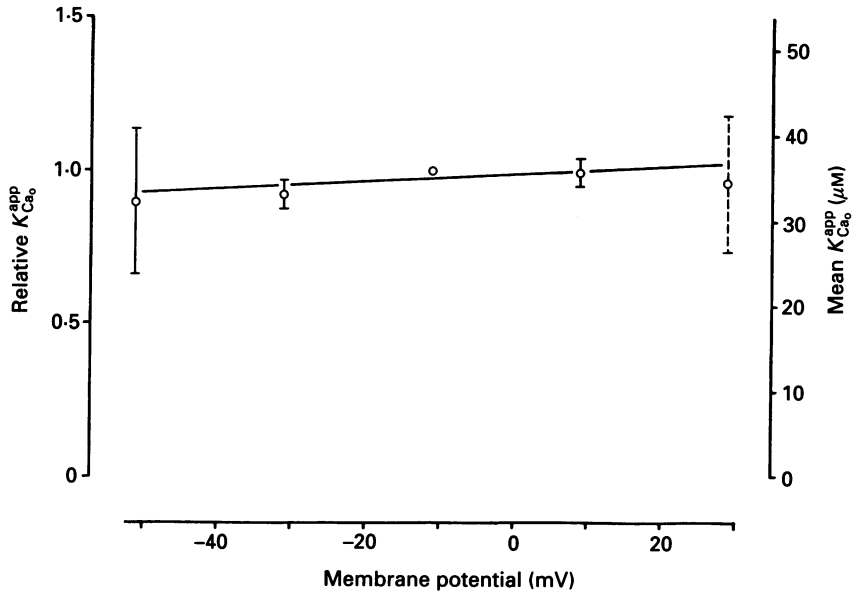

Fig. 6. Influence of membrane potential on the Ca_o^{2+} dependence of the reversed exchange current. Each $K_{Ca_o}^{app}$ measurement was expressed relative to the mean control $K_{Ca_o}^{app}$ measurement made at −11 mV in the same outer segment. Vertical scale on the right represents the best estimate of the mean $K_{Ca_o}^{app}$, obtained by multiplying the relative $K_{Ca_o}^{app}$ by 36 μM, the overall mean $K_{Ca_o}^{app}$ obtained at −11 mV in this population of outer segments. Vertical bars represent standard errors of mean estimates from three to four outer segments. Point at 29 mV represents mean estimate from two outer segments; dashed bar represents range. Includes data from a total of five outer segments. Straight line represents the function $K_{Ca_o}^{app} = 1{\cdot}31 \times 10^{-3}V + 0{\cdot}975$ where $K_{Ca_o}^{app}$ is given in μM and V_m is the membrane potential in mV.

conditions (e.g. a different membrane potential), although more than two points on the Ca_o^{2+} dependence curve were obtained if there had been a substantial change in $K_{Ca_o}^{app}$. Finally the same three exchange currents were recorded again under control conditions. The test estimate of $K_{Ca_o}^{app}$ is expressed as the relative $K_{Ca_o}^{app}$, i.e. the test estimate divided by the mean of the two control estimates. The best estimate of the absolute $K_{Ca_o}^{app}$ value under those test conditions can then be obtained by multiplying the mean relative $K_{Ca_o}^{app}$ by the overall mean $K_{Ca_o}^{app}$, i.e. 34 μM.

Estimates of the $K_{Ca_o}^{app}$ have been obtained in the presence of 20 mM K_o^+ at membrane potentials between −51 mV and +29 mV. As shown in Fig. 6, the relative $K_{Ca_o}^{app}$ shows little or no voltage dependence; the gradient of the straight line fitted to the data by linear regression is not significantly different from zero ($1{\cdot}3 \times 10^{-3} \pm 1{\cdot}7 \times 10^{-3}$ mV^{-1}, mean ± S.E.M. from five outer segments). This result shows that Ca_o^{2+} binds to a site which is outside the membrane electric field, and suggests that the Ca^{2+} translocation step is voltage independent (see Discussion).

$K^{app}_{Ca_o}$ was measured in the presence of 160 μM K^+_o (close to $K^{app}_{K_o}$, see below) with estimates obtained in 20 mM K^+_o both before and afterwards as controls. In the presence of 160 μM K^+_o, relative $K^{app}_{Ca_o}$ was $0{\cdot}56 \pm 0{\cdot}05$ (mean ± S.E.M. from five outer segments), giving an absolute $K^{app}_{Ca_o}$ value of 19 μM. K^+ ions, then, appear to compete

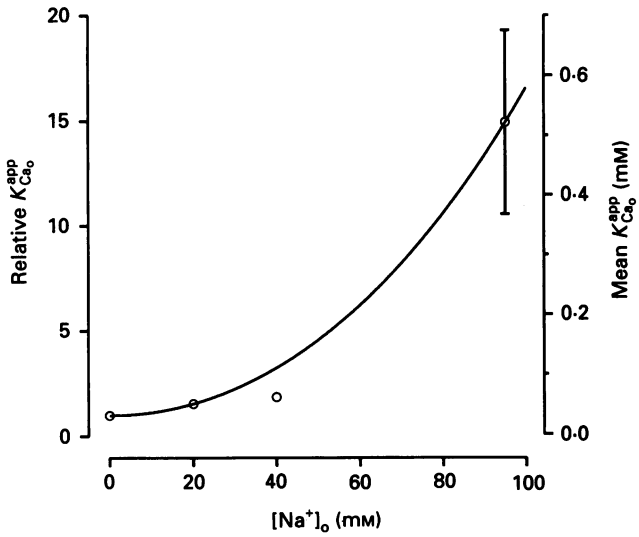

Fig. 7. Influence of Na^+_o on the Ca^{2+}_o dependence of the reversed exchange current. Each $K^{app}_{Ca_o}$ measurement was expressed relative to the mean control $K^{app}_{Ca_o}$ measurement made in the absence of Na^+_o. Vertical scale on the right represents the best estimate of the mean $K^{app}_{Ca_o}$, obtained by multiplying the relative $K^{app}_{Ca_o}$ by 35 μM, the overall mean $K^{app}_{Ca_o}$ obtained in 0 Na^+_o in this population of outer segments. Points at 20 mM and 40 mM Na^+_o each represent means from two measurements. Point at 95 mM Na^+_o represents mean from three outer segments, with standard error indicated by bar. Curve represents eqn (10) with $[K^+]_o$ = 20 mM, K_{Ca_o} = 56 μM, K_{x_o} = 17 mM and $K_{4_o}/\sqrt{L}$ = 27 mM.

with Ca^{2+} for exchange sites, in that reducing $[K^+]_o$ causes an increase in the apparent affinity for Ca^{2+}_o.

The same method was used to measure $K^{app}_{Ca_o}$ in the presence of 20 mM K^+_o and various concentrations of Na^+_o up to 95 mM. As shown in Fig. 7, Na^+_o appears to compete with Ca^{2+}_o for exchange sites, in that increasing $[Na^+]_o$ reduces the apparent affinity for Ca^{2+}_o. The continuous curve in Fig. 7 represents eqn (10) with $[K^+]_o$ = 20 mM, K_{Ca_o} = 56 μM, K_{x_o} = 17 mM and $K_{4_o}/\sqrt{L}$ = 27 mM (see Discussion). Note that the absence of Ca^{2+}_i in this experiment prevents any contribution of the forward mode of the exchange to the recorded current.

Influence of $[Ca^{2+}]_i$ on Ca^{2+}_o dependence

In their study of the ion dependence of the Na^+–Ca^{2+}, K^+ exchange in salamander rod outer segments, Hodgkin & Nunn (1987) found that the dependence of the exchange on Ca^{2+}_i was not affected by a reduction in Na^+_o from 110 to 55 mM. On this basis they adopted a 'one-step simultaneous' model of the exchange, a feature of which was that the ionic concentrations at the external face would not influence the apparent ionic affinities at the internal face of the exchange molecule, and vice versa.

The techniques used in the present study make it possible to test the validity of this type of model more rigorously, by observing whether the binding of Ca_o^{2+} and K_o^+ were influenced by $[Ca^{2+}]_i$

The method for studying the effect of $[Ca^{2+}]_i$ on the Ca_o^{2+} dependence of the exchange is illustrated in Fig. 8. The plot of the exchange current activated by a

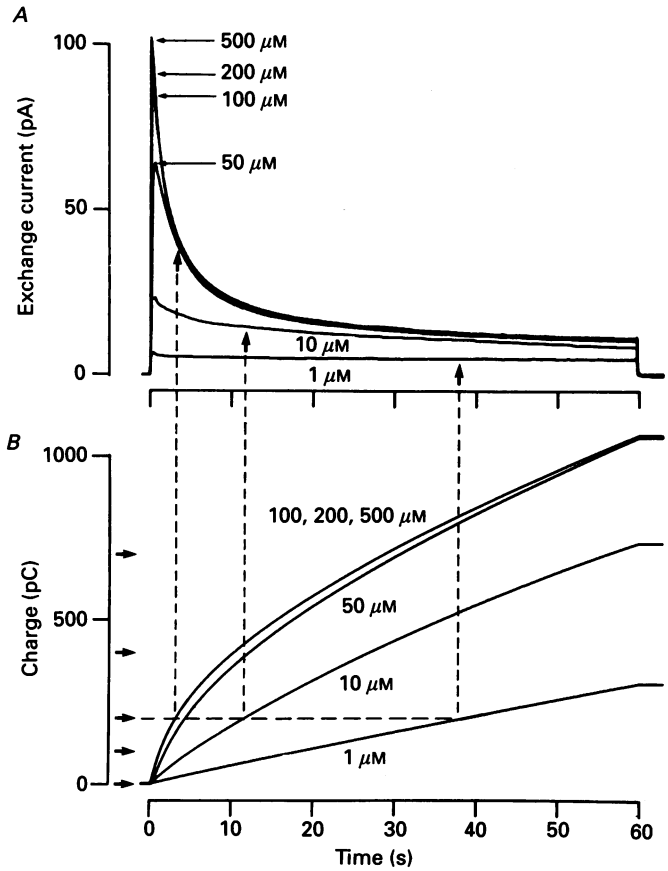

Fig. 8. Method for estimating $K_{Ca_o}^{app}$ at various concentrations of Ca_i^{2+}. *A*, family of exchange currents activated by various concentrations of Ca_o^{2+}, from Fig. 5*A*. *B*, series of charge traces obtained by integrating the traces shown in panel *A* with respect to time. Dotted lines illustrate method for a $[Ca^{2+}]_i$ equivalent to 200 pC: time taken for 200 pC to enter outer segment is read off each charge trace in panel *B*, and current recorded at this time is read off the corresponding current trace in panel *A*. See text for details.

given $[Ca^{2+}]_o$ (Fig. 8*A*) can be integrated to obtain the charge transferred as a function of time (Fig. 8*B*). We have assumed that a particular value of charge transferred corresponds for all traces to a constant free $[Ca^{2+}]_i$. This assumption depends on the following observations. (1) All of the outward current activated by the application of Ca_o^{2+} is carried by the Na^+–Ca^{2+}, K^+ exchange. The light-sensitive current has been suppressed in these experiments by the omission of GTP and cyclic GMP from the solution in the whole-cell pipette, and the exchange is the only other

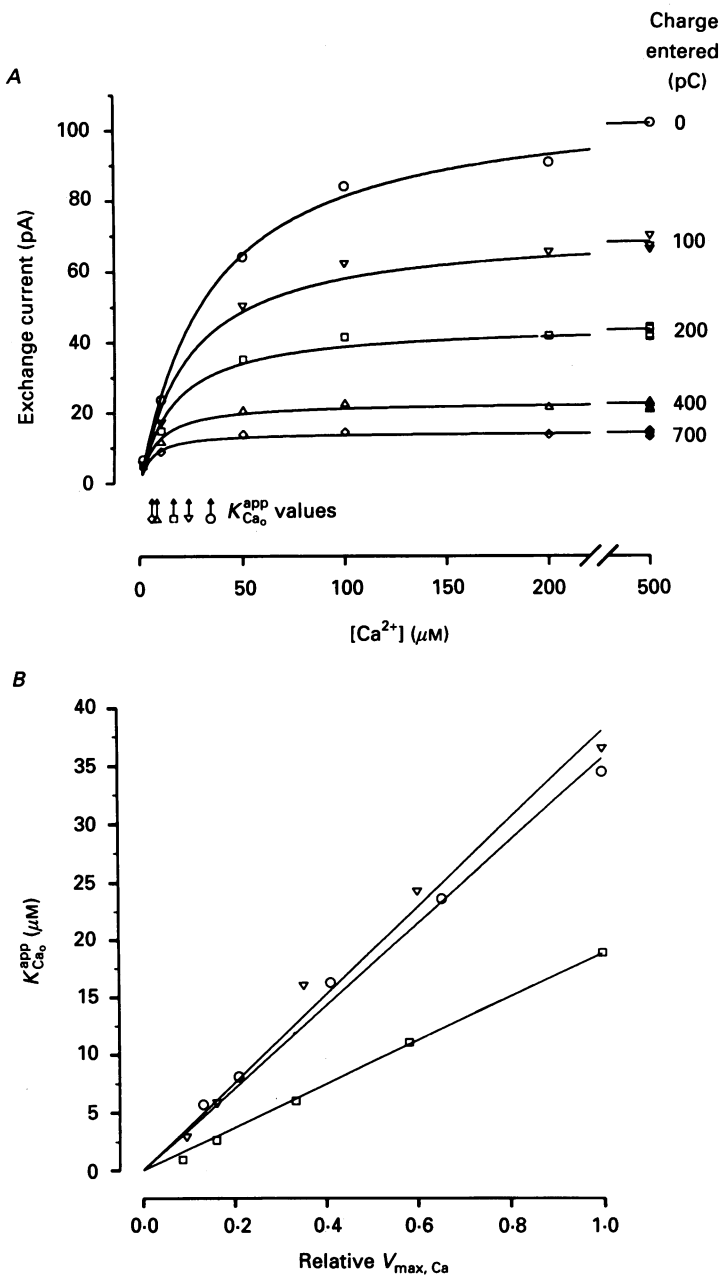

Fig. 9. Influence of $[Ca^{2+}]_i$ on the Ca_o^{2+} dependence of reversed exchange. *A*, series of Ca_o^{2+} dependence curves after various quantities of charge, as indicated on the right of each trace, have been transported by the exchange, i.e. at various fixed $[Ca^{2+}]_i$ levels. *B*, relationship between $K^{app}_{Ca_o}$ and relative $V_{max, Ca}$ for the outer segment shown in *A* (○) and two other outer segments.

electrogenic mechanism in the outer segment membrane (Lagnado & McNaughton, 1991). Figure 1, trace 1 shows that the addition of Ca_o^{2+} up to 0·5 mM causes no significant change in the junction current. (2) The exchange operates with a constant stoichiometry (see above). (3) The intracellular buffering of Ca^{2+} is instantaneous.

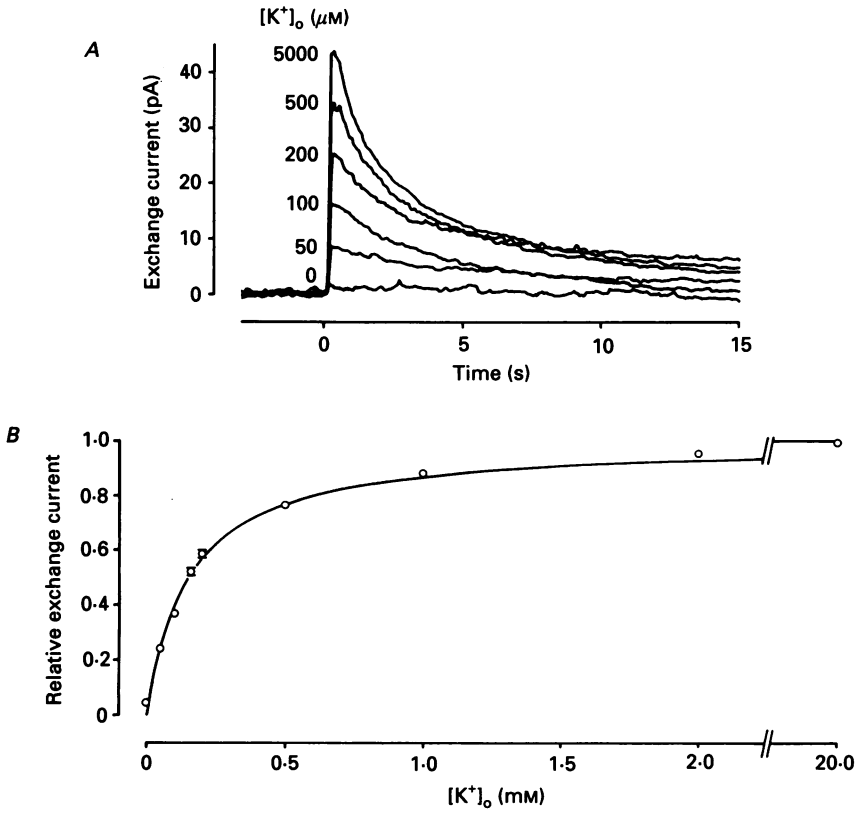

Fig. 10. K_o^+ dependence of reversed exchange current. *A*, series of exchange currents activated by addition of 0·5 mM Ca_o^{2+} in the presence of various concentrations of K_o^+. Traces have been aligned on the current axis so that the zero levels coincide. Holding potential, −11 mV. *B*, curve showing initial amplitude of exchange current as a function of $[K^+]_o$. Bars represent standard errors of mean estimates from three to six outer segments. Includes data from a total of nine outer segments. Continuous curve represents the Michaelis function: relative current = $[K^+]_o/(K_{K_o}^{app} + [K^+]_o)$. The curve of best fit, found using a least-squares curve-fitting routine (see Methods), gave $K_{K_o}^{app} = 151 \pm 3$ μM (mean ± S.E.M.).

Lagnado *et al.* (1992) showed that the buffering in the rod outer segment is non-linear but that no time dependence of the buffering is observed.

The Ca_o^{2+} dependence of the exchange at a constant free $[Ca^{2+}]_i$ can therefore be obtained from these traces. An example is shown by the dotted lines in Fig. 8 which illustrate the method for a charge entry of 200 pC, which in this outer segment of cytosolic volume 1·4 pl corresponds to a free $[Ca^{2+}]_i$ of 74 μM (calculated from eqn (8) of Lagnado *et al.* 1992 with $B = 16$ and $C = 240$ μM). The time taken for 200 pC to

enter the outer segment was read off each charge trace in Fig. 8*B*, and the current recorded at this time was then read off the corresponding current trace in Fig. 8*A*. The series of current values was used to construct a Ca_o^{2+} dependence curve for the exchange in the presence of this $[Ca^{2+}]_i$ level. A similar procedure was used to obtain

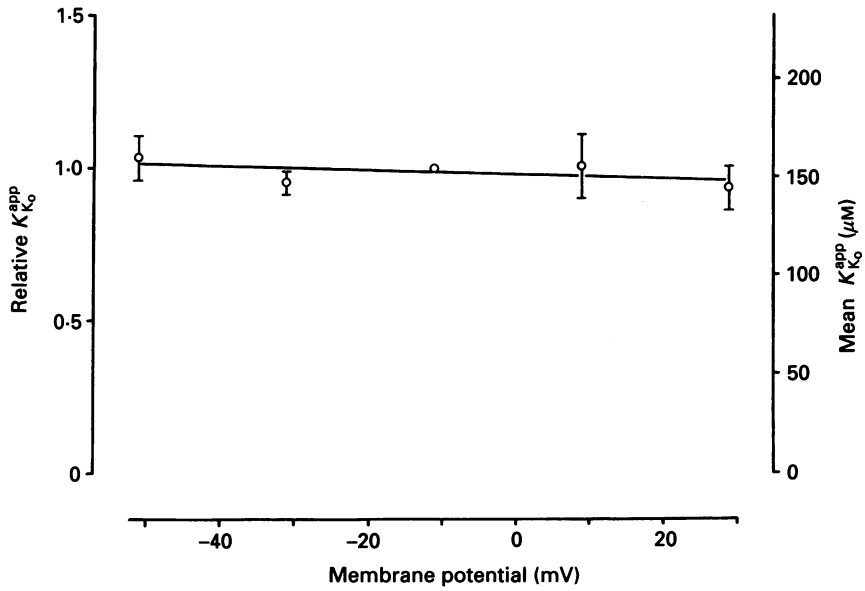

Fig. 11. Influence of membrane potential on the K_o^+ dependence of the reversed exchange current. Each $K_{K_o}^{app}$ measurement was expressed relative to the mean control $K_{K_o}^{app}$ measurement made at −11 mV in the same outer segment. Vertical scale on the right represents the best estimate of the mean $K_{K_o}^{app}$, obtained by multiplying the relative $K_{K_o}^{app}$ by 151 μM, the overall mean $K_{K_o}^{app}$ obtained at −11 mV in this population of outer segments. Each measurement (other than control) represents a mean from two outer segments; bars represent ranges. Includes data from a total of nine outer segments. Line represents the function $K_{K_o}^{app} = 0{\cdot}989 - 7{\cdot}40 \times 10^{-4} V_m$ where $K_{K_o}^{app}$ is given in μM and V_m is the membrane potential in mV.

Ca_o^{2+} dependence curves for the levels of $[Ca^{2+}]_i$ reached after the transport of 100, 400 and 700 pC of charge via reversed exchange.

In Fig. 9*A* the family of Ca_o^{2+} dependence curves so obtained has been plotted, with the quantity of charge which has been transported shown to the right of each curve. The $K_{Ca_o}^{app}$ of each curve is shown at the bottom of the figure. As the level of $[Ca^{2+}]_i$ rises, indicated by the increase in charge transferred, the V_{max} of the Ca_o^{2+} dependence curve, $V_{max,Ca}$, diminishes. At the same time the value of $K_{Ca_o}^{app}$ also diminishes, that is the apparent affinity of the exchange for Ca_o^{2+} appears to increase. Figure 9*B* shows, for the outer segment shown in Fig. 9*A* (○) and for two other outer segments, that $K_{Ca_o}^{app}$ and $V_{max,Ca}$ change in direct proportion to each other. A successful model of the exchange process should be able to reproduce this simple relationship.

Another way of expressing this observation is to say that at the origin of Fig. 9*A*, the gradient of each of the Ca_o^{2+} dependence curves is the same, since this gradient represents the ratio $V_{max,Ca}/K_{Ca_o}^{app}$. In other words, for small values of $[Ca^{2+}]_o$ the

exchange current does not depend on $[Ca^{2+}]_i$. This observation explains the absence of a transient component to the 1·μM Ca_o^{2+} trace in Fig. 5*A*: the accumulation of Ca_i^{2+} has almost no effect on the exchange current activated by such a small concentration of Ca_o^{2+}.

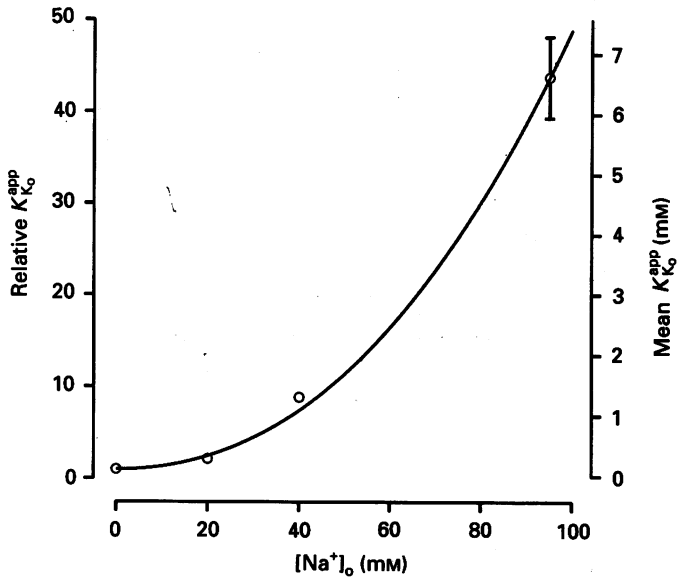

Fig. 12. Influence of Na_o^+ on the K_o^+ dependence of the reversed exchange current. Each $K_{K_o}^{app}$ measurement was expressed relative to the mean control $K_{K_o}^{app}$ measurement made in the absence of Na_o^+. Vertical scale on the right represents the best estimate of the mean $K_{K_o}^{app}$, obtained by multiplying the relative $K_{K_o}^{app}$ by 147 μM, the overall mean $K_{K_o}^{app}$ obtained in 0 Na_o^+ in this population of outer segments. Point at 20 mM Na_o^+ represents mean from two outer segments, point at 40 mM Na_o^+ represents a single measurement. Point at 95 mM Na_o^+ represents mean from three outer segments, with standard error indicated by bars. Curve represents eqn (11) with $[Ca^{2+}]_o = 0{\cdot}5$ mM, $K_{Ca_o} = 56$ μM, $K_{x_o} = 17$ mM and $K_{4_o}/\sqrt{L} = 27$ mM.

Dependence of the exchange on $[K^+]_o$

Figure 10*A* shows a series of reversed exchange currents, each of which was activated by the addition of 0·5 mM Ca_o^{2+}; the concentration of K_o^+ present during the solution change is indicated beside each trace. The trace labelled '0' shows that virtually no exchange current is activated by adding 0·5 mM Ca_o^{2+} in the absence of K_o^+, confirming the conclusion from Fig. 1 (trace 1) that the reversed mode of the exchange has an absolute requirement for K_o^+. Figure 10*B* shows that the activation of reversed exchange by K_o^+ is well described by a Michaelis relation with an apparent Michaelis constant, $K_{K_o}^{app}$, of 151 ± 3 μM (mean ± S.E.M., nine outer segments).

Influence of membrane potential, $[Ca^{2+}]_o$ *and* $[Na^+]_o$ *on* K_o^+ *dependence*

A procedure similar to that adopted for measuring $K_{Ca_o}^{app}$ over a wide range of conditions (see above) has been used to estimate $K_{K_o}^{app}$ in a similar range of conditions, obtaining two points on the Michaelis curve in conditions where $K_{K_o}^{app}$ appears to be

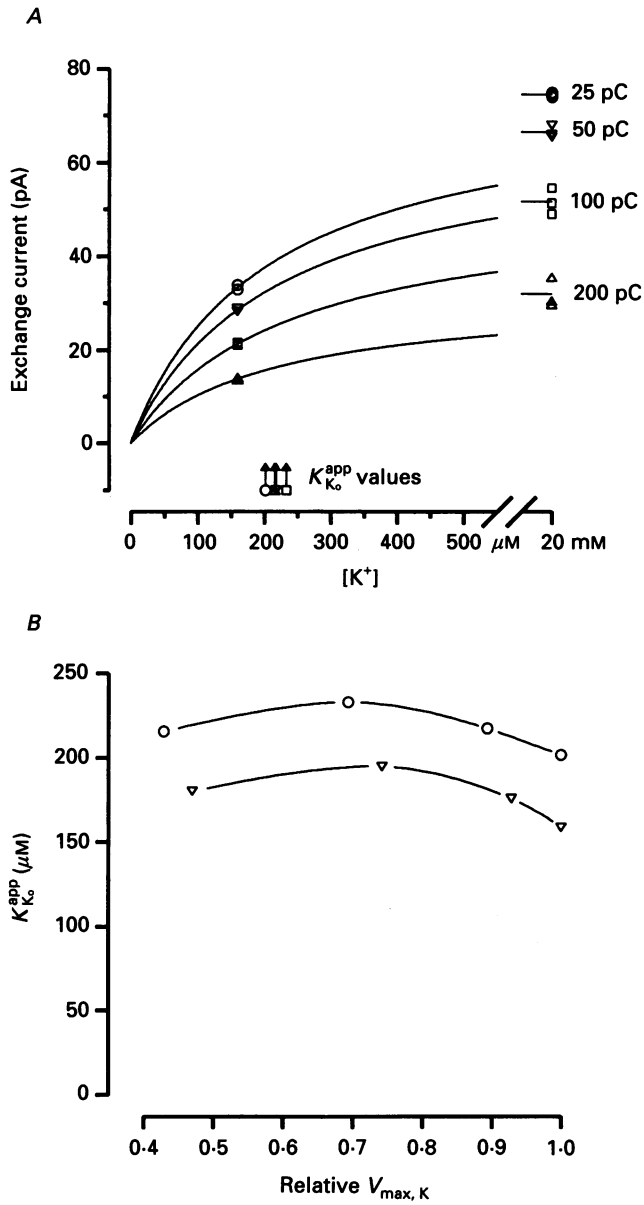

Fig. 13. Influence of $[Ca^{2+}]_i$ on the K_o^+ dependence of reversed exchange. *A*, series of K_o^+ dependence curves after various quantities of charge, as indicated on the right of each trace, have been transported by the exchange, i.e. at various fixed $[Ca^{2+}]_i$ levels. *B*, relationship between $K^{app}_{K_o}$ and relative $V_{max,K}$ for the outer segment shown in *A* (○) and one other outer segment. Curves have no theoretical significance.

very close to its control value, or three points when $K^{app}_{K_o}$ is markedly different from the control estimate (i.e. in 95 mM Na_o^+ and in reduced Ca_o^{2+}, see below). Estimates of the K_o^+ dependence of reversed exchange currents activated by 0·5 mM Ca_o^{2+} have been obtained at membrane potentials between −51 and +29 mV, as shown in Fig.

11. The $K_{K_o}^{app}$ shows little or no voltage dependence: the gradient of the regression line is not significantly different from zero ($-7{\cdot}4 \times 10^{-4} \pm 7{\cdot}6 \times 10^{-4}$ mV^{-1}, mean ± S.E.M. from three outer segments). This result shows that the K_o^+ binding site is like the Ca_o^{2+} binding site in that it lies outside the electric field of the membrane.

The effect of $[Ca^{2+}]_o$ on the K_o^+ dependence of the reversed exchange current was tested by comparing estimates of $K_{K_o}^{app}$ in 30 μM Ca_o^{2+} with control estimates obtained with 500 μM Ca_o^{2+}. With 30 μM Ca_o^{2+}, relative $K_{K_o}^{app}$ was 0·68 (mean from two outer segments), giving an absolute $K_{K_o}^{app}$ value of 102 μM. Thus K^+ and Ca^{2+} appear to compete in the activation of the reversed exchange current.

$K_{K_o}^{app}$ was also measured in the presence of up to 95 mM Na_o^+. As shown in Fig. 12, Na_o^+ appears to compete with K_o^+ for exchange sites, in that increasing $[Na^+]_o$ reduces the apparent affinity for K_o^+. The continuous curve in this figure represents eqn (11), with $[Ca^{2+}]_o = 0{\cdot}5$ mM, $K_{Ca_o} = 56$ μM, $K_{x_o} = 17$ mM and $K_{4_o}/\sqrt{L} = 27$ mM (see Discussion).

Influence of $[Ca^{2+}]_i$ on K_o^+ dependence

The method used to establish whether Ca_i^{2+} influences the K_o^+ dependence of the exchange was similar to the method applied earlier to obtain the effect of Ca_i^{2+} on the Ca_o^{2+} dependence. As shown in Fig. 13*A*, as Ca_i^{2+} accumulates, the K_o^+ dependence curve is compressed in its vertical axis without much effect on the horizontal axis, that is the V_{max} falls without very much effect on the $K_{K_o}^{app}$. Figure 13*B* shows $K_{K_o}^{app}$ as a function of $V_{max,K}$ for the outer segment in panel *A* (○) and one other outer segment. As $V_{max,K}$ falls, $K_{K_o}^{app}$ remains almost unaffected, in marked contrast with the fall in $K_{Ca_o}^{app}$ shown in Fig. 9*B*.

DISCUSSION

Stoichiometry of Na^+–Ca^{2+}, K^+ exchange

The experiments described in this paper show that little or no reversed exchange current was elicited in the absence of K_o^+, even when the outer segment membrane was exposed to a large outward Na^+ gradient and a large inward Ca^{2+} gradient. No Ca^{2+} entered the outer segment, showing that the exchange did not slip into an electroneutral mode such as $2Na^+$–$1Na^+$ in these conditions. Schnetkamp & Szerencsei (1991) demonstrated that release from K^+-depleted rod outer segments is stimulated by Na_o^+, and therefore argued that the exchange can proceed in the absence of K^+. This conclusion relies on the assumption that $[K^+]_i$ = zero in their K^+-depleted preparation. Although they show that the total $[K^+]_i$ is less than 5 μM, this does not place a maximum on the K^+ level in the compartment accessible to the exchange. Furthermore, the affinity of the exchange for internal K^+ may be even higher than at the external face, where in our conditions $K_{K_o}^{app}$ was 150 μM, so even a low $[K^+]_i$ may be sufficient to support a significant Ca^{2+} flux via K^+-dependent exchange.

Schnetkamp & Szerencsei (1991) also found that, at $[Ca^{2+}]_o$ levels above 150 μM, the Ca^{2+} influx into Na^+-loaded outer segments was only slightly reduced when $[K^+]_o$ was reduced from 10 mM to nominally zero. However, the nominally 0 K^+ solution did contain some K^+ (about 100 μM), carried over from the Ficoll gradient on which

the outer segments were purified, and this level of $[K^+]_o$ would be sufficient to produce a substantial activation of reversed exchange, given that in our experiments $K^{app}_{K_o}$ is 150 μM. Their conclusion that in the presence of high $[Ca^{2+}]_o$ the exchange can operate in a K^+-independent manner is contradicted by our observation that both the reversed exchange current and the associated Ca^{2+} influx were completely inhibited by removing K^+_o (see Fig. 1).

Models of the Na^+–Ca^{2+}, K^+ exchange

A considerable amount of information is now available about the various ion binding sites on the Na^+–Ca^{2+}, K^+ molecule, and about their interactions with one another and with membrane potential. The main observations which must be explained by a successful model of the exchange are as follows.

Observations on forward exchange (Na^+_o–Ca^{2+}_i, K^+_i)

(1) The rate of forward exchange is reduced e-fold by a 70 mV depolarization in Ringer solution, when the Na^+_o binding site is only partially occupied, but the rate becomes voltage independent with $[Na^+]_o$ = 220 mM and $[Ca^{2+}]_o = 0$, when the Na^+_o binding site is near saturation (Lagnado *et al.* 1988).

(2) Na^+_o activates forward exchange with a half-activation constant, $K_{\frac{1}{2}}$, of 93 mM and a Hill coefficient of 2·3 in the absence of other external ions and at a membrane potential of −14 mV (Lagnado *et al.* 1988).

(3) Ca^{2+}_i activates forward exchange in a first-order manner with a $K^{app}_{Ca_i}$ of 1·6 μM in near-physiological conditions (Lagnado *et al.* 1992).

(4) Na^+_i competes with Ca^{2+}_i for exchange binding sites, in that $K^{app}_{Ca_i}$ is increased by elevating $[Na^+]_i$ (Hodgkin & Nunn, 1987; Lagnado *et al.* 1992).

(5) $K^{app}_{Ca_i}$ is independent of $[Na^+]_o$ over the range 55–220 mM (Hodgkin & Nunn, 1987; Lagnado *et al.* 1988).

Observations on reversed exchange (Na^+_i–Ca^{2+}_o, K^+_o)

(6) The reversed exchange current is weakly voltage dependent, increasing e-fold with a 230 mV depolarization (Fig. 4). The effect of $[Na^+]_i$ on this voltage dependence was not investigated, but by analogy with the forward mode of the exchange (see observation (1)) the voltage dependence of reversed exchange may well be greater at low $[Na^+]_i$.

(7) The Ca^{2+}_o dependence of reversed exchange can be described by a Michaelis relation. The Michaelis constant, $K^{app}_{Ca_o}$, was 34 μM in the presence of 20 mM K^+_o (Fig. 5).

(8) The K^+_o dependence of reversed exchange can be described by a Michaelis relation. The Michaelis constant, $K^{app}_{K_o}$, was 151 μM in the presence of 0·5 mM Ca^{2+}_o (Fig. 10).

(9) Ca^{2+}_o and K^+_o appear to compete for the exchange: $K^{app}_{Ca_o}$ rises when $[K^+]_o$ is increased and $K^{app}_{K_o}$ rises when $[Ca^{2+}]_o$ is increased (pp. 455 and 462).

(10) Both $K^{app}_{Ca_o}$ and $K^{app}_{K_o}$ rise when $[Na^+]_o$ is increased (Figs 7 and 12).

(11) Neither $K^{app}_{Ca_o}$ nor $K^{app}_{K_o}$ is affected by membrane potential (Figs 6 and 11).

(12) When $[Ca^{2+}]_i$ is increased, $K^{app}_{Ca_o}$ falls in proportion with the V_{max}, but $K^{app}_{K_o}$ remains unaffected.

(13) Ca_i^{2+} inhibits reversed exchange in a first-order manner (p. 451 and Fig. 3).

These observations will be referred to by their numbers in the following discussion.

Classes of model considered and assumptions made in the analysis

There are three main classes of model for ion exchange processes; in the terminology adopted by Hilgemann (1989) these are the two-step simultaneous

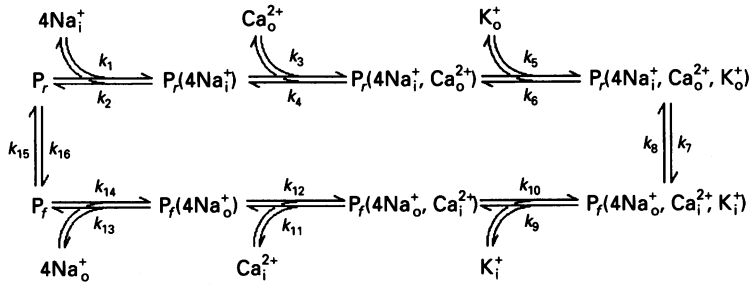

Fig. 14. Scheme for two-step simultaneous model of Na^+–Ca^{2+}, K^+ exchange. P_r and P_f represent the states of the exchanger which can bind the ions which participate in reversed and forward exchange respectively. Symbols shown in parentheses after P_r or P_f represent ions which are bound to the exchange molecule; k_1–k_{16} represent rate constants for the reactions shown. The Hill assumption has been made for the binding of Na_o^+ and Na_i^+, in that the proportions of exchange molecules with between one and three sodium ions bound is assumed to be zero. These states of the exchange are therefore not shown in the reaction scheme.

model, the one-step simultaneous model and the consecutive model. In the present analysis, we have chosen to keep the models as simple as possible by presupposing that any ion A can only influence the binding of another ion B by changing the availability of its binding site, not by modifying the intrinsic properties of that site. This influence may be exerted by a transmembrane gradient for ion A driving the binding sites for ion B onto the other side of the membrane by a mass action effect. Alternatively, ions may be constrained to bind in a particular order, e.g. A followed by B, so that the binding of ion A effectively uncovers binding sites for B.

Two-step simultaneous model

Figure 14 shows the exchange cycle of a simple two-step model of Na^+–Ca^{2+}, K^+ exchange. The term P_f represents a mode of the exchange which allows the binding of the ions which will participate in forward exchange (Na_o^+, Ca_i^{2+} and K_i^+) whereas P_r represents a mode of the exchange which will allow the binding of ions which will participate in reversed exchange (Na_i^+, Ca_o^{2+} and K_o^+). Symbols shown in brackets after these terms indicate ions which are bound to the exchange molecule.

The model is unusual, as compared with many models in the existing literature, in that the ions participating in reversed exchange must bind in the order Na_i^+, Ca_o^{2+} and then K_o^+. Since $[Na^+]_i$ remained constant throughout all of our experiments, the position(s) of the cycle at which Na_i^+ can bind does not affect the ability of the model to reproduce our results. For the sake of simplicity, Na_i^+ was assumed to bind at only one position on the exchange cycle, before Ca_o^{2+} or K_o^+.

The decision to constrain Ca_o^{2+} and K_o^+ to binding in a certain order, however, was not an arbitrary one. If the exchange cycle includes a state of the exchange which can bind either Ca_o^{2+} or K_o^+ in any order, then it follows that any change which increases the availability of the Ca_o^{2+} binding site must also increase the availability of the K_o^+ binding site to the same extent. The finding that an increase in $[Ca^{2+}]_i$ increases $K_{Ca_o}^{app}$ without having any effect on $K_{K_o}^{app}$ is therefore incompatible with such a model: Ca_o^{2+} and K_o^+ must be made to bind in one order or the other. The mathematical expression of this argument is developed for the ten-state consecutive model (see pp. 469 and 470).

A prediction of the two-step simultaneous model is that, at a constant membrane potential, the K_o^+ dependence of the exchange will have the form of a Michaelis relation in which the Michaelis constant, $K_{K_o}^{app}$ is given by the expression below, as derived in Appendix 1:

$$K_{K_o}^{app} = \frac{B(D + E\overline{Na_o^+} + \overline{Ca_o^{2+}})}{C(D + E\overline{Na_o^+}) + (A + F\overline{Na_o^+})\,\overline{Ca_o^{2+}}} K_{K_o}. \quad (6)$$

In this equation and in those which follow, $\overline{Ca_o^{2+}} = [Ca^{2+}]_o/K_{Ca_o}$ where $[Ca^{2+}]_o$ is expressed as millimolar and $\overline{Na_o^+} = ([Na^+]_o/K_{\frac{1}{2},Na_o})^h$ where $[Na^+]_o$ is expressed as millimolar. K_{Ca_o} and K_{K_o} are the dissociation constants (μM) which describe the binding of Ca_o^{2+} and K_o^+ to their binding sites on the exchange molecule, i.e. they are a fundamental property of the exchange. These constants should not be confused with $K_{Ca_o}^{app}$ and $K_{K_o}^{app}$, which represent the Michaelis constants measured from the Ca_o^{2+} and K_o^+ dependence curves of the exchange currents under a particular set of conditions (e.g. Figs 5*B* and 10*B*). $K_{\frac{1}{2},Na_o}$ is the concentration (mM) at which half of the Na^+ binding sites are occupied and h is the Hill coefficient for the binding of Na^+. *A*–*F* are positive constants as defined in Appendix 1.

In the absence of Na_o^+, it can be shown from eqn (6) that in order for $dK_{K_o}^{app}/d[Ca^{2+}]_o$ to be positive, as was seen experimentally (observation (9)), the inequality $C > A$ must be satisfied. However, in order for $dK_{K_o}^{app}/d[Ca^{2+}]_o$ to be positive, as was also seen experimentally (observation (10)), the inequality $A > C + (D + \overline{Ca_o^{2+}})F/E$ must be satisfied (see Appendix 1). These two conditions are mutually exclusive, and there are no simple modifications which can be introduced into the model, within the limits of the assumptions outlined above, which can overcome the inconsistency. For example, if K_o^+ binds before Ca_o^{2+} then the expression for $K_{Ca_o}^{app}$ is equivalent to the right-hand side of eqn (6) with $\overline{K_o^+}$ replaced by $\overline{Ca_o^{2+}}$ and K_{K_o} replaced by K_{Ca_o}. Now the model is inconsistent with the observations that $dK_{Ca_o}^{app}/d[K^+]_o$ and $dK_{Ca_o}^{app}/d[Na^+]_o$ are both positive (observations (9) and (10)).

One-step simultaneous model

The only difference between the one-step and two-step simultaneous models is that in the one-step model, there is a single state of the exchange, P, which can bind either the ions required to mediate forward exchange or those required to mediate reversed exchange. For the reason outlined above for the two-step model, it is necessary to constrain Ca_o^{2+} and K_o^+ to bind in a certain order, so the simplest example of this type of model is one with a reaction scheme identical to that in Fig. 14 except that the

subscripts r and f are removed, and P_r and P_f are replaced by a single state P, to which either Na_i^+ or Na_o^+ can bind. The expression for $K_{K_o}^{app}$ which is derived from this model is identical to that shown in eqn (6) except that there are small differences in the definitions of constants A, D, E and F (see Appendix 1). The one-step model

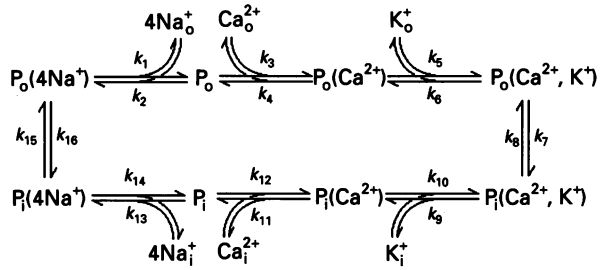

Fig. 15. Scheme for eight-state consecutive model of Na^+–Ca^{2+}, K^+ exchange. P_o and P_i represent the states of the exchanger which can bind external and internal ions respectively. Symbols shown in parentheses after P_o or P_i represent ions which are bound to the exchange molecule; k_1–k_{16} represent rate constants for the reactions shown.

therefore fails to explain the experimental results in exactly the same way as the two-step simultaneous model does. Simultaneous models of the exchange have therefore been abandoned.

Eight-state consecutive model

The simplest type of consecutive model of the exchange is an eight-state one, an example of which is shown in Fig. 15. As shown in Appendix 2, the model again predicts that, at constant membrane potential, the K_o^+ dependence of the exchange will have the form of a Michaelis function, but $K_{K_o}^{app}$ is now given by the equation:

$$K_{K_o}^{app} = \frac{B'(1+D'\overline{Na_o^+}+\overline{Ca_o^{2+}})}{C'(1+D'\overline{Na_o^+})+A'\overline{Ca_o^{2+}}}K_{K_o}. \tag{7}$$

A'–D' are positive constants as defined in Appendix 2 (note the similarity with constants A–D in Appendix 1), and other symbols are as previously defined. Using a method similar to that outlined in the previous section, it can be shown that in order for $dK_{K_o}^{app}/d[Ca^{2+}]_o$ to be positive, as observed in the absence of Na_o^+, the inequality $C' > A'$ must be satisfied. However, the observation that $dK_{K_o}^{app}/d[Na^+]_o$ is positive requires that $A' > C'$. As with the previous model, making K_o^+ bind before Ca_o^{2+} does not help, in that the model then becomes inconsistent with the findings that both $dK_{Ca_o}^{app}/d[K^+]_o$ and $dK_{Ca_o}^{app}/d[Na^+]_o$ are positive (see Appendix 2).

Ten-state consecutive model: interaction of Ca_o^{2+} and K_o^+

By contrast with the simultaneous models, the consecutive model can be salvaged relatively easily by introducing a slight modification. Figure 16 illustrates a ten-state model of the exchange, in which there are two sets of Na_o^+ binding sites. During

reversed exchange, as soon as the Na^+ translocation step has transferred the four Na^+ ions to the external surface, $(4-x)$ of these Na^+ ions can unbind (where x is an integer between 1 and 3). Ca_o^{2+} now binds to the exchange, converting it into a form which can release the remaining x Na^+ ions. Finally, K_o^+ binds to the exchange, converting

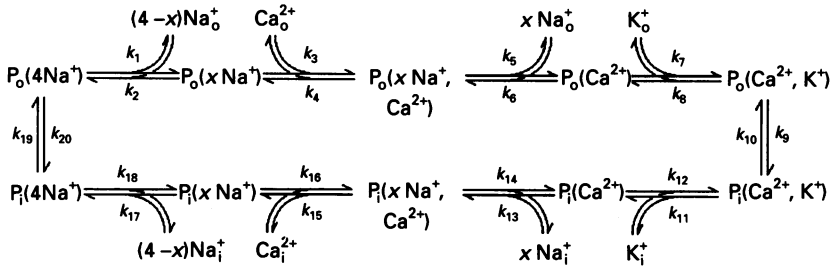

Fig. 16. Scheme for ten-state consecutive model of Na^+–Ca^{2+}, K^+ exchange. P_o and P_i represent the states of the exchanger which can bind external and internal ions respectively. Symbols shown in parentheses after P_o or P_i represent ions which are bound to the exchange molecule; k_1–k_{20} represent rate constants for the reactions shown.

it into a form which can translocate Ca^{2+} and K^+. The reverse series of reactions are assumed to proceed at the internal surface, yielding a state $P_i(4Na^+)$ which transfers $4Na^+$ to the external surface, thereby completing the exchange cycle.

As shown in Appendix 3, the model predicts that, at constant membrane potential and in the absence of Ca_i^{2+}, $K_{Ca_o}^{app}$ and $K_{K_o}^{app}$ will be given by the following equations:

$$K_{Ca_o}^{app} = \frac{(I\overline{K_o^+} + Jx\overline{Na_o^+})(1 + L\overline{4Na_o^+})}{G\overline{K_o^+} + J(1 + x\overline{Na_o^+})} K_{Ca_o}. \tag{8}$$

$$K_{K_o}^{app} = \frac{J\{\overline{Ca_o^{2+}} + x\overline{Na_o^+}(1 + \overline{Ca_o^{2+}} + L\overline{4Na_o^+})\}}{G\overline{Ca_o^{2+}} + I(1 + L\overline{4Na_o^+})} K_{K_o}. \tag{9}$$

G–L are positive constants, as defined in Appendix 3. $\overline{4Na_o^+} = ([Na^+]_o/K_{4_o})^H$ and $xNa_o^+ = ([Na^+]_o/K_{x_o})^h$, where $[Na^+]_o$ is expressed as millimolar, K_{4_o} and H represent the $K_{\frac{1}{2}}$ (mM) and Hill coefficient with which Na_o^+ binds to the sites which are available before Ca_o^{2+} binding, and K_{x_o} and h represent the $K_{\frac{1}{2}}$ and Hill coefficient for the Na_o^+ binding sites which are available after Ca_o^{2+} binds. Other symbols are as previously defined.

From eqns (8) and (9) it will be apparent that the observations that, in zero Na_o^+, $dK_{Ca_o}^{app}/d[K^+]_o$ and $dK_{K_o}^{app}/d[Ca^{2+}]_o$ are both positive follow directly from the model and do not impose any constraints upon it. The inclusion of Na_o^+ binding in two steps therefore frees the model of the inconsistency which made it necessary to reject the previous models. The adoption of a model in which Ca_o^{2+} must bind before K_o^+ follows from the observed effect of Ca_i^{2+} on $K_{Ca_o}^{app}$ and $K_{K_o}^{app}$, as explained in a later section.

In 0 $[Na^+]_o$ and 20 mM $[K^+]_o$, $K_{Ca_o}^{app}$ was found to be 34 μM, and in 0 $[Na^+]_o$ and 0·5 mM $[Ca^{2+}]_o$, $K_{K_o}^{app}$ was estimated to be 151 μM. These data can be inserted into eqns

(8) and (9), which can be used as simultaneous equations to show that $IK_{Ca_o}/G = 34\ \mu M$ and $JK_{K_o}/G = 162\ \mu M$. Equations (8) and (9) can therefore be rewritten as

$$K_{Ca_o}^{app} = \frac{(34[K^+]_o + 162\overline{xNa_o^+}K_{Ca_o})(1 + L\overline{4Na_o^+})}{[K^+]_o + 162(1 + \overline{xNa_o^+})}. \quad (10)$$

$$K_{K_o}^{app} = \frac{162\{\overline{Ca_o^{2+}} + \overline{xNa_o^+}(1 + \overline{Ca_o^{2+}} + L\overline{4Na_o^+})\}}{\overline{Ca_o^{2+}} + 34(1 + L\overline{4Na_o^+})/K_{Ca_o}}. \quad (11)$$

In 0 $[Na^+]_o$ these equations can be simplified to

$$K_{Ca_o}^{app} = \frac{34}{1 + 162/[K^+]_o}. \quad (12)$$

$$K_{K_o}^{app} = \frac{162}{1 + 34/[Ca^{2+}]_o}. \quad (13)$$

A prediction of this model, then, is that in the presence of 160 μM K_o^+, $K_{Ca_o}^{app} = 17\ \mu M$. Our experimental estimate obtained from five outer segments was 19 μM. The predicted value for $K_{K_o}^{app}$ in the presence of 30 μM Ca_o^{2+} is 75 μM. Our experimental estimate, from two outer segments, was 100 μM. Equations (12) and (13) are therefore consistent with our observations on the interaction between the binding of Ca_o^{2+} and the binding of K_o^+.

Ten-state model: effect of $[Na^+]_o$

Just as it was possible to use the data on the mutual influence of Ca_o^{2+} and K_o^+ binding to simplify eqns (8) and (9) to obtain eqns (10) and (11), so it should be possible to use the data on the influence of Na_o^+ on $K_{Ca_o}^{app}$ and $K_{K_o}^{app}$ to introduce further simplifications. The two classes of Na_o^+ binding site in the model make this complicated, but the mathematics can be simplified by assuming that $x = 2$, i.e. that two Na^+ bind at each position on the exchange cycle, and that $H = h = 2$, i.e. that the Hill coefficient is 2 in each case. This assumption is broadly consistent with previous results which show that the apparent Hill coefficient with which Na_o^+ activates forward exchange is approximately 2 (Lagnado *et al.* 1988; Schnetkamp & Szerencsei, 1991).

The data sets $[K^+]_o = 20$ mM, $[Na^+]_o = 95$ mM, $K_{Ca_o}^{app} = 510\ \mu M$ and $[K^+]_o = 20$ mM, $[Na^+]_o = 20$ mM, $K_{Ca_o}^{app} = 53\ \mu M$ can be inserted into eqn (10), and each of the resulting equations rearranged to give

$$K_{Ca_o} = \frac{\{6{\cdot}5(K_x)^2 + 510\}(K_4)^2/L - 4200(K_x)^2}{95^2 + (K_4)^2/L}. \quad (14)$$

$$K_{Ca_o} = \frac{\{5{\cdot}3(K_x)^2 + 52{\cdot}6\}(K_4)^2/L - 4200(K_x)^2}{20^2 + (K_4)^2/L}. \quad (15)$$

In addition, a further equation can be obtained by inserting the data set $[Ca^{2+}]_o = 0{\cdot}5$ mM, $[Na^+]_o = 95$ mM, $K_{K_o}^{app} = 6{\cdot}6$ mM into eqn (11), which can then be rearranged to give

$$K_{Ca_o} = \frac{\{2{\cdot}4(K_x)^2 - 500\}(K_4)^2/L - 1400(K_x)^2}{95^2 + (K_4)^2/L}. \quad (16)$$

Equations (14)–(16) can be combined to obtain solutions for the three unknowns K_{Ca_o}, K_x and $K_4/\sqrt{L}$. The values which are obtained are $K_{Ca_o} = 56\ \mu M$, $K_x = 17$ mM and $K_4/\sqrt{L} = 27$ mM. These are the values which have been inserted back into eqns (10) and (11) to generate the continuous curves shown in Figs 7 and 12.

Ten-state model: effect of Ca_i^{2+}

The next question to address is whether the model is consistent with the surprising result that increasing $[Ca^{2+}]_i$ reduces $K^{app}_{Ca_o}$ without affecting $K^{app}_{K_o}$ (observation (12)). As shown in Appendix 3, in 0 Na_o^+ the characteristics of the Ca_o^{2+} dependence of the exchange are

$$K^{app}_{Ca_o} = \frac{I}{G + J/\overline{K_o^+} + (N + P/\overline{K_o^+})\,\overline{Ca_i^{2+}}} K_{Ca_o}, \tag{17}$$

$$V_{max,\,Ca} = \frac{1}{G + J/\overline{K_o^+} + (N + P/\overline{K_o^+})\,\overline{Ca_i^{2+}}}, \tag{18}$$

where $V_{max,\,Ca}$ is the V_{max} of the Ca_o^{2+} dependence curve, G, I, J, N and P are positive constants as defined in Appendix 3, and other symbols are as previously defined. Dividing eqn (17) by eqn (18) gives $K^{app}_{Ca_o}/V_{max,\,Ca} = IK_{Ca_o}$. A prediction of the model, then, is that $K^{app}_{Ca_o}$ and $V_{max,\,Ca}$ will both diminish as $[Ca^{2+}]_i$ increases, but $K^{app}_{Ca_o}/V_{max,\,Ca}$ will remain constant. As Fig. 9*B* shows, this prediction is borne out by the experimental data.

The characteristics of the K_o^+ dependence curve, also derived in Appendix 3, are as follows:

$$K^{app}_{K_o} = \frac{J + P\overline{Ca_i^{2+}}}{G + I/\overline{Ca_o^{2+}} + N\overline{Ca_i^{2+}}}, \tag{19}$$

$$V_{max,\,K} = \frac{1}{G + I/\overline{Ca_o^{2+}} + N\overline{Ca_i^{2+}}}, \tag{20}$$

with symbols as previously defined. The prediction is that as $[Ca^{2+}]_i$ increases, $V_{max,\,K}$ will diminish, as is observed. The effect of $[Ca^{2+}]_i$ on $K^{app}_{K_o}$, however, will depend on the values of the constants in eqn (19). The experiments showed that as $[Ca^{2+}]_i$ increased, there was little change in $K^{app}_{K_o}$ (observation (10)), and this result is reproduced by eqns (19) and (20) provided $(G + I/\overline{Ca_o^{2+}})P \approx JN$. All of our observations on the ion dependence of reversed exchange, then, are consistent with the ten-state model illustrated in Fig. 16.

Which binds first, Ca_o^{2+} or K_o^+?

As mentioned in the previous section, it follows from the model illustrated in Fig. 16 that as $[Ca^{2+}]_i$ increases, $K^{app}_{Ca_o}$ and $V_{max,\,Ca}$ should both be reduced in such a way that $K^{app}_{Ca_o}/V_{max,\,Ca}$ remains constant, as was observed experimentally (observation (12)). If Ca_o^{2+} and K_o^+ exchanged places in Fig. 16, then it would necessarily follow from the model that as $[Ca^{2+}]_i$ is increased, $K^{app}_{K_o}$ and $V_{max,\,K}$, the V_{max} of the K_o^+ dependence curve, would diminish in such a way that $K^{app}_{K_o}/V_{max,\,K}$ would remain in proportion. This is clearly incompatible with our finding that as $[Ca^{2+}]_i$ rises, $V_{max,\,K}$

falls whilst $K_{K_o}^{app}$ remains virtually unchanged. Within the context of these types of models, then, our results imply that Ca_o^{2+} binds to the exchange before K_o^+ in the reversed exchange cycle.

From Fig. 16 it would be expected that K_o^+–K_i^+ exchange can occur without involving Ca^{2+}, but Ca_o^{2+}–Ca_i^{2+} exchange cannot occur without an equimolar quantity

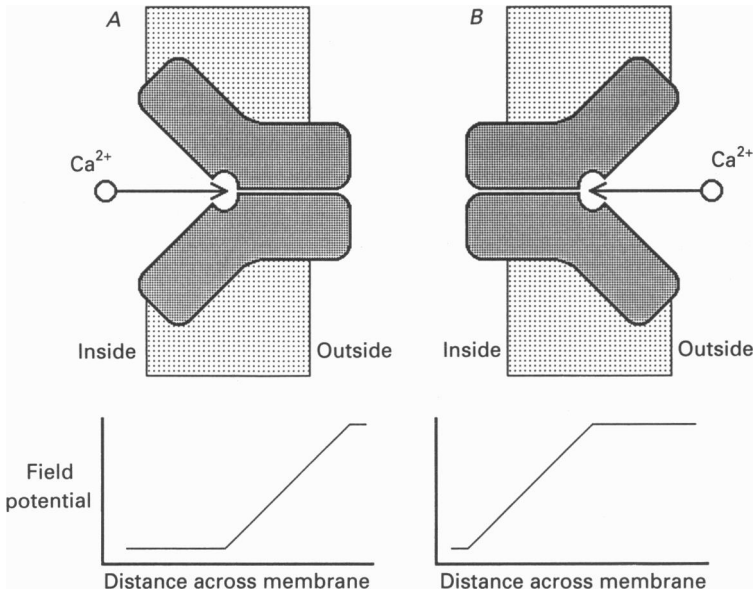

Fig. 17. Model to explain the voltage independence of the binding of Ca^{2+} on both sides of the membrane. *A*, gate on outside of membrane closed, and change in potential distributed entirely across this gate. *B*, gate on inside of membrane closed, and change in potential distributed entirely across this gate. Note that the Ca^{2+} ion does not sense any of the membrane potential whether it binds from the inside or from the outside.

of K^+ also being transported. In conditions where both of these self-exchange modes can operate, then, the exchange should transport at least as much K^+ as Ca^{2+}. Schnetkamp *et al.* (1991) showed that when Rb_o^+ and Sr_o^+ act as substitutes for K_o^+ and Ca_o^{2+} in stimulating the simultaneous release of K^+ and Ca^{2+} from outer segments, K_i^+ is initially released more rapidly than Ca_i^{2+}. This result supports our conclusion: it is consistent with a consecutive model in which Ca^{2+} binds to the exchange before K^+, but inconsistent with a model in which K^+ binds first.

Voltage independence of Ca_o^{2+} and K_o^+ binding

There are two possible explanations for the voltage dependence of the apparent Michaelis constant or $K_{\frac{1}{2}}$ with which a cation activates the exchange. The first is that the binding of the ion to its site is voltage dependent, as is the case if the site lies within the membrane electric field, so that the ion must cross a proportion of the membrane field before it binds. Depolarization will tend to drive the cation out of its site, decreasing the effective concentration at the site and so decreasing the effective affinity of the cation for the exchange (see Lagnado *et al.* 1988). A second possibility

is that the membrane potential reversibly influences the number of sites available to bind the cation. Depolarization may draw a negatively charged cation binding site away from the external surface, so that a larger concentration of the cation would be required to achieve the same transport rate, i.e. the apparent affinity would decrease.

In the present study we found that both $K_{Ca_o}^{app}$ and $K_{K_o}^{app}$ were independent of the membrane potential over a wide range (−59 to +29 mV). This result implies that, for both Ca_o^{2+} and K_o^+, neither the binding of the ion to its site nor the availability of its binding sites are affected by the membrane potential; the only alternative is the unlikely possibility that binding and availability have equal and opposite voltage dependence and that these two effects exactly cancel out. Lagnado *et al.* (1988) observed that the Ca_i^{2+} dependence of forward Na^+–Ca^{2+}, K^+ exchange also does not depend on membrane potential, implying that the Ca_i^{2+} binding site on the inner surface of the exchange molecule is also outside the membrane field.

A model which would explain these observations is illustrated in Fig. 17, which illustrates only the Ca^{2+} binding part of the exchange molecule. According to this scheme, Ca^{2+} binds to a single fixed site within the exchange molecule, between two 'gates', only one of which is open at any one time. When the inner gate is open (Fig. 17*A*), the whole of the membrane field is distributed across the outer gate, so that the binding of Ca_i^{2+} is voltage independent. When the outer gate opens and the inner gate closes (Fig. 17*B*), the whole membrane field would need to be distributed across the inner gate, in order that Ca_o^{2+} can bind in a voltage-independent manner.

No charge transfer accompanying translocation of Ca^{2+} and K^+

One complete exchange cycle involves the translocation of a single positive charge, whether the exchange is operating in forward or reversed mode (see p. 448). During reversed exchange either the Na^+ translocation step or the Ca^{2+}, K^+ translocation step carries one net positive charge out of the outer segment, or else both translocation steps carry charge, with an overall net outward transfer of one positive charge.

If the Ca^{2+}, K^+ translocation step is accompanied by a net transfer of charge across the membrane, then the membrane potential would be expected to influence the availability of the binding sites for Ca_o^{2+}, or K_o^+, or both of these ions. Either $K_{Ca_o}^{app}$ or $K_{K_o}^{app}$ or both would be expected to be voltage dependent. In our model of the exchange, for example, it is apparent from eqn (9) that $K_{K_o}^{app}$ is proportional to the quantity J, which is a constant at a fixed membrane potential. As explained in Appendix 3, if the Ca^{2+}, K^+ translocation step is voltage dependent, J (and therefore $K_{K_o}^{app}$) can only remain independent of the membrane potential if the unbinding of K_o^+ is extremely slow relative to the other steps in the exchange cycle. Since the mechanism must allow K_o^+ to unbind during forward exchange, the mode in which it normally operates, it is unlikely that this step is so slow, and much more likely that the Ca^{2+}, K^+ translocation step is voltage independent.

Charge transfer during Na^+ translocation?

If the charge is not transferred during the Ca^{2+}, K^+ translocation step, then it must be transferred during the Na^+ translocation step, implying that this step is voltage

dependent. In this section we address the question of whether a voltage-dependent Na^+ translocation step is sufficient to explain all of the available data, or whether other steps must also be voltage dependent. As shown in Appendix 3, the ten-state model predicts that the current generated by forward Na^+–Ca^{2+}, K^+ exchange ($-j$), in the absence of Ca_o^{2+}, is given by the equation:

$$-\frac{1}{j} = Q + \frac{I + R\overline{K_o^+}}{x\overline{Na_o^+}} + \frac{1}{\overline{Ca_i^{2+}}}\left(T + \frac{U}{4\overline{Na_o^+}}\right)\left(W + \frac{X\overline{K_o^+}}{x\overline{Na_o^+}}\right), \tag{21}$$

where Q–X are positive constants defined in Appendix 3, with other symbols as previously defined.

Lagnado *et al.* (1988) found that at low $[Na^+]_o$ values the exchange was voltage dependent, but when $[Na^+]_o$ was raised to 220 mM, the exchange became almost voltage independent (observation (1)). Their experiments were conducted in the absence of Na_i^+ so, as shown in Appendix 3, eqn (21) can be simplified to

$$-\frac{1}{j} = Q + \frac{I + R\overline{K_o^+}}{x\overline{Na_o^+}} + \frac{W}{\overline{Ca_i^{2+}}}. \tag{22}$$

If the exchange is voltage dependent in low $[Na^+]_o$ but voltage independent in high $[Na^+]_o$, then $Q + W/\overline{Ca_i^{2+}}$ must be voltage independent and $(I + R\overline{K_o^+})K_{x_o}$ must be voltage dependent. In the absence of Na_i^+, $(I + R\overline{K_o^+})K_{x_o}$ may be expanded as $[1 + \{1 + (1 + 1/\overline{K_i^+})/K^t_{Ca,K}\}\overline{K_o^+}](k_5/k_4 + 1/k_6)/k_6$, where $K^t_{Ca,K} = k_{10}/k_9$. The only terms in this expression which can confer the required voltage dependence on the overall value are k_5 and k_6; all of the other terms are likely to be voltage independent, for the following reasons. (a) Since Ca_o^{2+} binds in a voltage-independent fashion (observation (11)), k_4 must be voltage independent. (b) It seems reasonable to assume that $\overline{K_i^+}$ is voltage independent, as outlined in point (iii) in the next section. (c) As discussed earlier, it seems likely that the equilibrium constant of the Ca^{2+}, K^+ translocation step, $K^t_{Ca,K}$, is voltage independent (see p. 471).

This result indicates that the voltage dependence of the Na^+ translocation step is not sufficient to explain a voltage dependence of forward exchange which is abolished in high $[Na^+]_o$, as was observed by Lagnado *et al.* (1988). In addition, the binding or unbinding of xNa^+ in Fig. 16 (with rate constants k_6 and k_5 respectively), or both of these, must also be voltage dependent. This might result from a voltage-dependent conformational change in the xNa^+ binding site. An alternative explanation is that Na^+ ions might bind to sites within the membrane and sense part of the membrane field as they bind, as suggested by Lagnado *et al.* (1988). In this case, at a given fixed concentration of Na^+ in the bulk solution (i.e. a fixed $[Na^+]_o$ in our equations), a hyperpolarization would increase the effective $[Na^+]$ at the site and so increase the rate of Na^+ binding (represented by $k_6[Na^+]_o$). According to this idea, then, the rate constant of Na^+ binding, k_6, would be voltage dependent.

Overall voltage dependence of reversed exchange

The experiments described in this study show that the voltage dependence of the reversed exchange current over the range -51 to $+29$ mV is most simply described as an e-fold increase in current for every 230 mV depolarization (observation (6)). Most of the steps shown in Fig. 16 can be ruled out as possible contributors to the

overall voltage dependence as follows. (i) The binding of external ions does not contribute to the voltage dependence: Na_o^+ was absent in the voltage-dependence experiments, and Ca_o^{2+} and K_o^+ binding were both found to be voltage independent. (ii) A voltage-dependent inhibition of reversed exchange by Ca_i^{2+} is ruled out since the voltage-dependence measurements were made on initial ($[Ca^{2+}]_i = 0$) reversed exchange currents. (iii) A voltage-dependent inhibition of the exchange by K_i^+ seems unlikely. If K_i^+ sensed part of the membrane potential as it bound, a depolarization would drive K^+ into the binding site, enhancing the inhibition of reversed exchange. Depolarization would therefore decrease the exchange current, whereas an increase is observed experimentally (observation (6)). (iv) The Ca^{2+} and K^+ translocation step is probably voltage independent, since Ca_o^{2+} and K_o^+ both bind in a voltage-independent manner (see above). Two possible sources of voltage dependence remain. Firstly, as argued above, it seems likely that the Na^+ translocation step is voltage dependent. Secondly, the binding of Na_i^+ to the exchange may be voltage dependent; this might be expected by analogy with the voltage dependence of the Na_o^+ binding site, but there is no direct evidence for or against it at present.

Why, then, is the voltage dependence of reversed exchange which we measured (an e-fold change in 230 mV) so much weaker than the voltage dependence of forward exchange measured by Lagnado *et al.* (1988; an e-fold change in 70 mV)? Lagnado *et al.* (1988) activated forward exchange with 110 mM Na_o^+ in the presence of 1 mM Ca_o^{2+}, whereas we activated reversed exchange with 129 mM Na_i^+, with the absence of Ca_i^{2+} making the effective $[Na^+]$ even higher. This greater saturation of the Na_i^+ binding sites may partially explain the weaker voltage dependence which we observed (see observation (1)).

Influence of $[Na^+]_o$ on Ca_i^{2+} dependence of forward Na^+–Ca^{2+}, K^+ exchange

Hodgkin & Nunn (1987) rejected consecutive models of the exchange because they observed that changing $[Na^+]_o$ from 110 to 55 mM, in conditions which were otherwise approximately physiological, had little or no effect on the Ca_i^{2+} dependence of forward Na^+–Ca^{2+}, K^+ exchange in whole rods (observation (5)). Lagnado *et al.* (1988) confirmed this result over the $[Na^+]_o$ range 55–220 mM in voltage-clamped rod outer segments. Equation (21), which was derived assuming 0 Ca_o^{2+} as used by Lagnado *et al.* (1988), can be rearranged into the form of a Michaelis relation in which the Michaelis constant $K_{Ca_i}^{app}$ is given by

$$K_{Ca_i}^{app} = \frac{(T\overline{4Na_o^+} + U)\,(W\overline{xNa_o^+} + X\overline{K_o^+})}{(I + R\overline{K_o^{2+}} + Qx\overline{Na_o^+})\,\overline{4Na_o^+}} K_{Ca_i}. \tag{23}$$

There are several ways in which $K_{Ca_i}^{app}$ could be effectively independent of $[Na^+]_o$ over a range of 55–220 mM. A simple example is obtained if it is assumed that $\overline{4Na_o^+}$ is much greater than U/T and $I/\overline{K_o^+} + R \approx QX/W$, in which case $K_{Ca_i}^{app}$ will be independent of $[Na^+]_o$. Note that in the experiments of Lagnado *et al.* (1988), in which $[Na^+]_i$ and $[K^+]_o$ were both zero, the independence from $[Na^+]_o$ is obtained if $\overline{xNa_o^+}$ is much greater than I/Q.

Summary of models of Na^+–Ca^{2+}, K^+ exchange

Of the models considered for the Na^+–Ca^{2+}, K^+ exchange mechanism, the one-step simultaneous model fails to explain the observed dependence of $K_{Ca_o}^{app}$ on $[Ca^{2+}]_i$ (observation (12)); and the two-step simultaneous and eight-state consecutive models (shown in Figs 14 and 15) cannot reproduce the observations that increasing either $[K^+]$ or $[Na^+]$ causes a rise in $K_{Ca_o}^{app}$ and that increasing $[Ca^{2+}]$ or $[Na^+]$ causes a rise in $K_{K_o}^{app}$ (observations (9) and (10)). The ten-state model of the exchange (shown in Fig. 16), however, can reproduce all of these results, although Ca^{2+} must bind to the exchange before K^+ in order to reproduce the finding that when Ca_i^{2+} increases, $K_{Ca_o}^{app}$ is reduced without any change in $K_{K_o}^{app}$.

The observation that neither $K_{Ca_o}^{app}$ nor $K_{K_o}^{app}$ is influenced by the membrane potential (observation (11)) strongly suggests that the Ca^{2+} and K^+ translocation step is voltage independent, i.e. that the single charge which crosses the membrane during one cycle of the exchange is probably transferred during the Na^+ translocation step.

The abolition of the voltage dependence of forward exchange in the presence of high $[Na^+]_o$ (observation (1), Lagnado *et al.* 1988) suggests that the binding of Na_o^+ to the exchange (at the position marked by k_6 in Fig. 16) is also voltage dependent. This result could be explained either by the Na^+ ions sensing part of the membrane field as they bind or by a voltage-dependent conformational change in the Na^+ binding site.

Finally, the ten-state model in which Ca^{2+} binds to the exchange before all Na^+ ions have unbound suggests how the Na^+–Ca^{2+}, K^+ exchange might be related to the Na^+–Ca^{2+} exchange found in most other tissues. We have for simplicity assumed in our ten-state model that two Na^+ ions leave before Ca^{2+} binding, followed by two which leave before K^+ binding, but a model in which three Na^+ ions must leave before Ca^{2+} binding, followed by a further Na^+ ion which dissociates before K^+ binding, is equally consistent with the experimental observations. The first process would then take place much as in the Na^+–Ca^{2+} exchange. The subsequent loss of the final Na^+ ion and binding of the single K^+ ion might take place on a distinct and possibly phylogenetically more recent region of the exchange molecule.

This work was supported by the MRC and NATO.

APPENDIX 1

Two-step simultaneous model (zero $[Ca^{2+}]_i$)

Figure 14 gives the scheme for the operation of this model of the exchange. P_r and P_f represent the states of the exchanger which can bind the ions which participate in reversed and forward exchange respectively. Symbols shown in parentheses after P_r or P_f represent ions which are bound to the exchange molecule; k_1–k_{16} represent rate constants for the reactions shown. The Hill assumption has been made for the binding of Na_o^+ and Na_i^+, in that the number of exchange molecules with between one and three sodium ions bound is assumed to be zero. These states of the exchange are therefore not shown in the reaction scheme. It is assumed that Na^+ binds externally and internally with the same Hill coefficient, H.

The rate of unbinding of Ca_i^{2+} is given by $k_{11}P_f(4Na_o^+, Ca_i^{2+})$, where k_{11} is the rate constant for the reaction and $P_f(4Na_o^+, Ca_i^{2+})$ is the number of the exchange molecules in the state in which only external Na^+ and internal Ca^{2+} have bound. The net flux through each of the other seven reactions in the exchange cycle is given by the rate of the reversed exchange reaction (represented in Fig. 14 by arrows pointing in a clockwise direction) minus the forward (anticlockwise) rate. With the exchange at steady state and in the absence of Ca_i^{2+}, each of these net fluxes is equated with the rate of unbinding of Ca_i^{2+} to give the following seven equations:

$$k_{11}P_f(4Na_o^+, Ca_i^{2+}) = k_9P_f(4Na_o^+, Ca_i^{2+}, K_i^+) - k_{10}[K^+]_iP_f(4Na_o^+, Ca_i^{2+}), \quad (24)$$

$$k_{11}P_f(4Na_o^+, Ca_i^{2+}) = k_7P_r(4Na_i^+, Ca_o^{2+}, K_o^+) - k_8P_f(4Na_o^+, Ca_i^{2+}, K_i^+), \quad (25)$$

$$k_{11}P_f(4Na_o^+, Ca_i^{2+}) = k_5[K^+]_oP_r(4Na_i^+, Ca_o^{2+}) - k_6P_r(4Na_i^+, Ca_o^{2+}, K_o^+), \quad (26)$$

$$k_{11}P_f(4Na_o^+, Ca_i^{2+}) = k_3[Ca^{2+}]_oP_r(4Na_i^+) - k_4P_r(4Na_i^+, Ca_o^{2+}), \quad (27)$$

$$k_{11}P_f(4Na_o^+, Ca_i^{2+}) = k_1([Na^+]_i)^HP_r - k_2P_r(4Na_i^+), \quad (28)$$

$$k_{11}P_f(4Na_o^+, Ca_i^{2+}) = k_{15}P_f - k_{16}P_r, \quad (29)$$

$$k_{11}P_f(4Na_o^+, Ca_i^{2+}) = k_{13}P_f(4Na_o^+) - k_{14}([Na^+]_o)^HP_f. \quad (30)$$

Equation (24) is rearranged to give:

$$P_f(4Na_o^+, Ca_i^{2+}, K_i^+) = \frac{k_{11}+k_{10}[K^+]_i}{k_9}P_f(4Na_o^+, Ca_i^{2+}).$$

This equation is substituted into eqn (25), which is then rearranged to give $P_r(4Na_i^+, Ca_o^{2+}, K_o^+)$ as a multiple of $P_f(4Na_o^+, Ca_i^{2+})$. This process is continued, with eqns (26)–(30), until the numbers of molecules in each of the states of the exchange $P_f(4Na_o^+)$, P_f, P_r, $P_r(4Na_i^+)$, $P_r(4Na_i^+, Ca_o^{2+})$, $P_r(4Na_i^+, Ca_o^{2+}, K_o^+)$ and $P_f(4Na_o^+, Ca_i^{2+}, K_i^+)$, are all expressed as multiples of $P_f(4Na_o^+, Ca_i^{2+})$ with coefficients which are complex combinations of k_1–k_{20}, $[Ca^{2+}]_i$, $[K^+]_i$, $([Na^+]_i)^H$, $[Ca^{2+}]_o$, $[K^+]_o$ and $([Na^+]_o)^H$. It is assumed that Na^+ binds externally and internally with the same Hill coefficient, H.

The units of the rate constants can be chosen so that the current (in pA) flowing through the exchange, j, is given by k_{11} multiplied by the proportion of exchange molecules in the state $P_f(4Na_o^+, Ca_i^{2+})$, i.e. $j = k_{11}P_f(4Na_o^+, Ca_i^{2+})/P_{tot}$ where $P_{tot} = P_f(4Na_o^+, Ca_i^{2+}) + P_f + P_f(4Na_o^+) + P_r + P_r(4Na_i^+) + P_r(4Na_i^+, Ca_o^{2+}) + P_r(4Na_i^+, Ca_o^{2+}, K_o^+) + P_f(4Na_o^+, Ca_i^{2+}, K_i^+)$. P_{tot} can be expressed as a multiple of $P_f(4Na_o^+, Ca_i^{2+})$, and this expression is divided by $k_{11}P_f(4Na_o^+, Ca_i^{2+})$, to give an equation for the exchange current of the form:

$$\frac{1}{j} = A + \frac{B}{\overline{K_o^+}} + \frac{B/\overline{K_o^+}+C}{\overline{Ca_o^{2+}}}(D + E\overline{Na_o^+}) + F\overline{Na_o^+}, \quad (31)$$

where $A = 1/k_7 + 1/k_{11} + 1/k_{13} + (1+K^t_{Na,Ca,K})(1/k_9 + \overline{K_i^+}/k_{11}) + 1/k_2\overline{Na_i^+} + F$; $B = 1/k_6 + 1/k_7 + (1/k_9 + \overline{K_i^+}/k_{11})K^t_{Na,Ca,K}$; $C = 1/k_4$; $D = 1 + 1/\overline{Na_i^+} + E$; $E = K^t/\overline{Na_i^+}$ and $F = 1/k_{15} + E/k_2$. $\overline{Ca_o^{2+}} = [Ca^{2+}]_o/K_{Ca_o}$ where $K_{Ca_o} = k_4/k_3$; $\overline{K_o^+} = [K^+]_o/K_{K_o}$ where $K_{K_o} = k_6/k_5$; $\overline{Na_o^+} = ([Na^+]_o/K_{\frac{1}{2},Na_o})^H$ where $K_{\frac{1}{2},Na_o} = k_{13}/k_{14}$; $\overline{K_i^+} = [K^+]_i/K_{K_i}$ where $K_{K_i} = k_9/k_{10}$; and $\overline{Na_i^+} = ([Na^+]_i/K_{\frac{1}{2},Na_i})^H$ where $K_{\frac{1}{2},Na_i} = k_2/k_1$. $K^t_{Na,Ca,K} = k_8/k_7$ and

$K^t = k_{16}/k_{15}$. This equation may be rearranged to show j as a function of $[K^+]_o$. The resulting equation has the form of a Michaelis relation with a Michaelis constant, $K^{app}_{K_o}$, which is given by the equation:

$$K^{app}_{K_o} = \frac{B(D+E\overline{Na_o^+}+\overline{Ca_o^{2+}})}{C(D+E\overline{Na_o^+})+(A+F\overline{Na_o^+})\,\overline{Ca_o^{2+}}}K_{K_o}. \tag{32}$$

This equation is given in the main text as eqn (6). By differentiating with respect to Ca_o^{2+}, it is shown that in the absence of Na_o^+:

$$\frac{dK^{app}_{K_o}}{d\overline{Ca_o^{2+}}} = \frac{BD(C-A)}{CD+A\overline{Ca_o^{2+}}}K_{K_o}. \tag{33}$$

Since A–D, K_{K_o} and $\overline{Ca_o^{2+}}$ are all positive, in order for the model to be consistent with the experimental observation that $dK^{app}_{K_o}/d\overline{Ca_o^{2+}}$ is positive, the inequality $C > A$ must be satisfied. On the other hand, if eqn (32) is differentiated with respect to $\overline{Na_o^+}$, the following equation is obtained:

$$\frac{dK^{app}_{K_o}}{d\overline{Na_o^+}} = \frac{\{(A-C)E-(D+\overline{Ca_o^{2+}})F\}B\overline{Ca_o^{2+}}}{\{(CD+A\overline{Ca_o^{2+}})+(CE+F\overline{Ca_o^{2+}})\,\overline{Na_o^+}\}^2}K_{K_o}. \tag{34}$$

In order for the model to be consistent with the observation that $dK^{app}_{K_o}/d\overline{Na_o^+}$ is positive, the inequality $A > C+(D+\overline{Ca_o^{2+}})F/E$ must be satisfied. This requirement is incompatible with the experimental observation that $dK^{app}_{K_o}/d\overline{Ca_o^{2+}}$ is positive, as shown above.

One-step simultaneous model (zero $[Ca^{2+}]_i$)

The scheme for the operation of this model of the exchange is identical to that shown in Fig. 14 except that subscripts r and f are removed and the states P_r and P_f are replaced by a single state, P, to which either Na_i^+ or Na_o^+ may bind. The equation for the exchange current has the same form as eqn (31), with constants as defined above except that $A = 1/k_7+1/k_{11}+1/k_{13}+(1+K^t_{Na,Ca,K})(1/k_9+\overline{K_i^+}/k_{11})+1/k_2\overline{Na_i^+}$; $D = 1+1/\overline{Na_i^+}$; $E = 1/\overline{Na_i^+}$ and $F = 1/k_2\overline{Na_i^+}$.

APPENDIX 2

Eight-state consecutive model (zero $[Ca^{2+}]_i$)

The scheme showing the operation of this model of the exchange is given as Fig. 15. As before, k_1–k_{16} represent rate constants for the reactions shown. P_o and P_i represent the states of the exchange with ion binding sites exposed to the external and internal media respectively. The ions which are bound to each state of the exchange are shown in parentheses. By a method similar to that adopted in Appendix 1, it can be shown that

$$\frac{1}{j} = A'+\frac{B'}{\overline{K_o^+}}+\frac{B'/\overline{K_o^+}+C'}{\overline{Ca_o^{2+}}}(1+D'\overline{Na_o^+}), \tag{35}$$

where $A' = 1/k_7+1/k_{11}+1/k_{15}+(1+K^t_{Ca,K})(1/k_9+\overline{K_i^+}/k_{11})+(1+K^t_{Na})/k_1+(1/k_{14}+$

$1/k_{15}+K^t_{Na}/k_1)/\overline{Na_i^+}$; $B'=1/k_6+1/k_7+(1/k_9+\overline{K_i^+}/k_{11})K^t_{Ca,K}$; $C'=1/k_4$; $D'=1+K^t_{Na}(1+1/\overline{Na_i^+})$. $\overline{Ca_o^{2+}}=[Ca^{2+}]_o/K_{Ca_o}$ where $K_{Ca_o}=k_4/k_3$; $\overline{K_o^+}=[K^+]_o/K_{K_o}$ where $K_{K_o}=k_6/k_5$; $\overline{Na_o^+}=([Na^+]_o/K_{\frac{1}{2},Na_o})^H$ where $K_{\frac{1}{2},Na_o}=k_1/k_2$; $\overline{Ca_i^{2+}}=[Ca^{2+}]_i/K_{Ca_i}$ where $K_{Ca_i}=k_{11}/k_{12}$; $\overline{K_i^+}=[K^+]_i/K_{K_i}$ where $K_{K_i}=k_9/k_{10}$; and $\overline{Na_i^+}=([Na^+]_i/K_{\frac{1}{2},Na_i})^H$ where $K_{\frac{1}{2}}=k_{14}/k_{13}$. $K^t_{Ca,K}=k_8/k_7$ and $K^t_{Na}=k_{16}/k_{15}$. This equation may be rearranged to show j as a function of $[K^+]_o$. The resulting equation has the form of a Michaelis relation with a Michaelis constant, $K^{app}_{K_o}$, given by

$$K^{app}_{K_o}=\frac{B'(1+D'\overline{Na_o^+}+\overline{Ca_o^{2+}})}{C'(1+D'\overline{Na_o^+})+A'\overline{Ca_o^{2+}}}K_{K_o}. \tag{36}$$

This equation is given in the main text as eqn (7). By differentiating with respect to Ca_o^{2+} we obtain:

$$\frac{K^{app}_{K_o}}{d\overline{Ca_o^{2+}}}=\frac{B'(C'-A')(1+D'\overline{Na_o^+})}{\{C'(1+D'\overline{Na_o^+})+A'\overline{Ca_o^{2+}}\}^2}K_{K_o}. \tag{37}$$

Since A'–D' and $\overline{Ca_o^{2+}}$ are all positive, in order for the model to be consistent with the experimental observation that $dK^{app}_{K_o}/d\overline{Ca_o^{2+}}$ is positive, the inequality $C'>A'$ must be satisfied. On the other hand, if eqn (36) is differentiated with respect to $\overline{Na_o^+}$, the following equation is obtained:

$$\frac{dK^{app}_{K_o}}{d\overline{Na_o^+}}=\frac{B'D'(A'-C')\overline{Ca_o^{2+}}}{\{A'\overline{Ca_o^{2+}}+C'(1+D'\overline{Na_o^+})\}^2}. \tag{38}$$

In order for the model to be consistent with the observation that $dK^{app}_{K_o}/d\overline{Ca_o^{2+}}$ is positive, the inequality $A'>C'$ must be satisfied. This requirement is incompatible with the experimental observation that $dK^{app}_{K_o}/d\overline{Ca_o^{2+}}$ is positive, as shown above.

APPENDIX 3

Ten-state consecutive model

The scheme for the operation of this model of the exchange is given as Fig. 16. As before, k_1–k_{20} represent rate constants for the reactions shown. P_o and P_i represent the states of the exchange with ion binding sites exposed to the external and internal media respectively. The ions which are bound to each state of the exchange are shown in parentheses. The letter x represents an integer between 1 and 3. Na^+ is assumed to bind to $P_o(xNa^+)$ and $P_i(xNa^+)$ with the same Hill coefficient, H, and to bind to $P_o(Ca^{2+})$ and $P_i(Ca^{2+})$ with the same Hill coefficient, h.

Reversed exchange, zero $[Ca^{2+}]_i$

In the absence of Ca_i^{2+}, the rate of unbinding of Ca_i^{2+} is given by $k_{15}P_i(xNa^+, Ca^{2+})$, and this is equated with the net flux through each of the other steps to obtain nine equations. Using a method similar to that described in Appendix 1, these equations are used to obtain expressions for the quantity of each state of the exchanger, each in the form of a coefficient multiplied by $P_i(xNa^+, Ca^{2+})$. As before, the rate constants are given units such that fluxes are expressed as exchange currents (in pA). To obtain an expression for the current, j, through the exchange, $k_{15}P_i(xNa^+, Ca^{2+})$ is divided

by the total number of exchange molecules, i.e. the sum of all ten of the expressions for the quantities of each exchange state. This procedure yields the following equation for j, the exchange current:

$$\frac{1}{j} = G + \frac{I}{\overline{Ca_o^{2+}}}(1 + L\overline{4Na_o^+}) + \frac{J}{\overline{K_o^+}}\left\{1 + \overline{xNa_o^+}\left(1 + \frac{1 + L\overline{4Na_o^+}}{\overline{Ca_o^{2+}}}\right)\right\}, \tag{39}$$

where $G = (1 + K^t_{Na})/k_1 + 1/k_5 + 1/k_8 + 1/k_9\, k_{11}(1 + K^t_{Ca,K}) + 1/k_{15} + 1/k_{19} + (1/k_{14} + 1/k_{15})\{1 + (1 + K^t_{Ca,K})\overline{K_i^+}\}/\overline{xNa_i^+}$; $I = 1/k_4 + 1/k_5$; $J = 1/k_8 + \{1/k_{10} + 1/k_{11} + (1/k_{14} + 1/k_{15})\,\overline{K_i^+}/\overline{xNa_i^+}\}K^t_{Ca,K}$; and $L = 1 + K^t_{Na}(1 + 1/\overline{4Na_i^+})$. $\overline{Ca_o^{2+}} = [Ca^{2+}]_o/K_{Ca_o}$ where $K_{Ca_o} = k_4/k_3$; $\overline{K_o^+} = [K^+]_o/K_{K_o}$ where $K_{K_o} = k_8/k_7$; $\overline{4Na_o^+} = ([Na^+]_o/K_{4_o})^H$ where $K_{4_o} = k_1/k_2$; and $\overline{xNa_o^+} = ([Na^+]_o/K_{x_o})^h$ where $K_{x_o} = k_5/k_6$; $\overline{K_i^+} = [K^+]_i/K_{K_i}$ where $K_{K_i} = k_{11}/k_{12}$; and $\overline{Na_i^+} = [Na^+]_i/K_{\frac{1}{2},Na_i}$ where $K_{\frac{1}{2},Na_i} = k_{14}/k_{13}$. $K^t_{Ca,K} = k_{10}/k_9$ and $K^t_{Na} = k_{20}/k_{19}$. Equation (39) may be rearranged to show j as a function of $[Ca^{2+}]_o$, and this manoeuvre shows that the equation has the form of a Michaelis relation with a Michaelis constant, $K^{app}_{Ca_o}$, which is given by

$$K^{app}_{Ca_o} = \frac{(I\overline{K_o^+} + J\overline{xNa_o^+})(1 + L\overline{4Na_o^+})}{G\overline{K_o^+} + J(1 + \overline{xNa_o^+})}K_{Ca_o}. \tag{40}$$

This equation is given in the main text as eqn (8). Alternatively eqn (40) can be arranged to show the j as a function of $[K^+]_o$, in which case it has the form of a Michaelis relation with a Michaelis constant, $K^{app}_{K_o}$, which is given by

$$K^{app}_{K_o} = \frac{J\{\overline{Ca_o^{2+}} + \overline{xNa_o^+}(1 + \overline{Ca_o^{2+}} + L4Na_o^+)\}}{G\overline{Ca_o^{2+}} + I(1 + L\overline{4Na_o^+})}K_{K_o}. \tag{41}$$

This equation is given in the main text as eqn (9). It will be apparent from the definition of J, given above, that if the Ca^{2+}, K^+ translocation step (represented by $K^t_{Ca,K}$) is voltage dependent, then J can only remain independent of membrane potential if $1/k_8$ is much greater than $\{1/k_{10} + 1/k_{11} + (1/k_{14} + 1/k_{15})\,\overline{K_i^+}/\overline{xNa_i^+}\}K^t_{Ca,K}$, i.e. if the unbinding of K_o^+ is much slower than the other steps in the exchange cycle.

Reversed exchange, zero $[Na^+]_o$

In the absence of Na_o^+, the rate of unbinding of Na_o^+ is given by $k_5 P_o(xNa^+, Ca^{2+})$, and this is equated with the net flux through each of the other steps to obtain nine equations. Using a method similar to that described in Appendix 1, these equations are used to obtain expressions for the quantity of each state of the exchange, each in the form of a coefficient multiplied by $P_o(xNa^+, Ca^{2+})$. To obtain an expression for the exchange current, j, $k_5 P_o(xNa^+, Ca^{2+})$ is divided by the total number of exchange molecules, i.e. the sum of all ten of the expressions for the quantities of each exchange state. This procedure yields the following equation:

$$\frac{1}{j} = G + \frac{I}{\overline{Ca_o^{2+}}} + \frac{J}{\overline{K_o^+}} + \left(N + \frac{P}{\overline{K_o^+}}\right)\overline{Ca_i^{2+}}, \tag{42}$$

where $N = [1 + \{1 + (1 + K^t_{Ca,K})\,\overline{K_i^+}\}/\overline{xNa_i^+}]M$ and $P = K^t_{Ca,K}K_i^+ M/\overline{xNa_i^+}$, with $M = (1/k_{18} + 1/k_{19} + K^t_{Na}/k_1)/\overline{4Na_i^+}$ and other constants are as previously defined. Equation (42) may be rearranged to show the current, j, as a function of $[Ca^{2+}]_o$.

The resulting equation has the form of a Michaelis relation with a Michaelis constant, $K^{app}_{Ca_o}$, and a V_{max}, $V_{max,Ca}$, which are given by the following expressions:

$$K^{app}_{Ca_o} = \frac{I}{G + J/\overline{K_o^+} + (N + P/\overline{K_o^+})\,\overline{Ca_i^{2+}}} K_{Ca_o}, \tag{43}$$

$$V_{max,Ca} = \frac{1}{G + J/\overline{K_o^+} + (N + P/\overline{K_o^+})\,\overline{Ca_i^{2+}}}. \tag{44}$$

These equations are given in the main text as eqns (17) and (18). Alternatively eqn (42) can be arranged to show j as a function of $[K^+]_o$, in which case it has the form of a Michaelis relation with a Michaelis constant, $K^{app}_{K_o}$, and a V_{max}, $V_{max,K}$, which are given by

$$K^{app}_{K_o} = \frac{J + P\overline{Ca_i^{2+}}}{G + I/\overline{Ca_o^{2+}} + N\overline{Ca_i^{2+}}}, \tag{45}$$

$$V_{max,K} = \frac{1}{G + I/\overline{Ca_o^{2+}} + N\overline{Ca_i^{2+}}}. \tag{46}$$

These equations are given in the main text as eqns (19) and (20).

Forward exchange, zero $[Ca^{2+}]_o$

Using a method similar to that in Appendix 1 it is possible to obtain an equation for the current generated by forward exchange, $-j$, in the absence of Ca_o^{2+}, which has the following form:

$$-\frac{1}{j} = Q + \frac{I + R\overline{K_o^+}}{x\overline{Na_o^+}} + \frac{1}{\overline{Ca_i^{2+}}}\left(T + \frac{U}{4\overline{Na_o^+}}\right)\left(W + \frac{X\overline{K_o^+}}{x\overline{Na_o^+}}\right), \tag{47}$$

where $I = 1/k_4 + 1/k_5$ as before, $Q = 1/k_4 + 1/k_8 + 1/k_{14} + 1/k_{20} + (1 + 1/K^t_{Na})/k_{18} + \{1 + (1 + x\overline{Na_i^+})/K_i^+\}\{1/k_{10} + 1/k_{11} + 1/k_8 K^t_{Ca,K}\}$; $R = [1 + \{1 + (1 + x\overline{Na_i^+})/K_i^+\}/K^t_{Ca,K}]I$; $T = \{1 + (1 + 1/K^t_{Na})\,4\overline{Na_i^+}\}$; $U = 4\overline{Na_i^+}/K^t_{Na}$; $W = 1/k_{14} + 1/k_{15} + (1/k_{10} + 1/k_{11} + 1/k_8 K^t_{Ca,K})\,x\overline{Na_i^+}/\overline{K_i^+}$; $X = (1/k_4 + 1/k_5)\,x\overline{Na_i^+}/\overline{K_i^+}/K^t_{Ca,K}$; and $\overline{Ca_i^{2+}} = [Ca_i^{2+}]/K_{Ca_i}$ where $K_{Ca_i} = k_{15}/k_{16}$ with other symbols as previously defined. This equation appears in the main text as eqn (21).

In the experiments of Lagnado *et al.* (1988), $[Na^+]_i$ = zero, and therefore the constants Q, R and W can be rewritten as $Q = 1/k_4 + 1/k_8 + 1/k_{14} + 1/k_{20} + (1 + 1/K^t_{Na})/k_{18} + \{1 + 1/K_i^+\}\{1/k_{10} + 1/k_{11} + 1/K^t_{Ca,K}/k_8\}$; $R = \{1 + 1/K^t_{Ca,K}(1 + 1/\overline{K_i^+})\}I$; $W = 1/k_{14} + 1/k_{15}$; whilst T, U and X acquire the values $T = 1$; $U = 0$; and $X = 0$. Equation (47) may therefore be simplified to

$$-\frac{1}{j} = Q + \frac{I + R\overline{K_o^+}}{x\overline{Na_o^+}} + \frac{W}{\overline{Ca_i^{2+}}}. \tag{48}$$

This equation appears in the main text as eqn (22).

REFERENCES

BAYLOR, D. A., LAMB, T. D. & YAU, K.-W. (1979). The membrane current of single rod outer segments. *Journal of Physiology* **288**, 589–611.

CERVETTO, L., LAGNADO, L., PERRY, R. J., ROBINSON, D. W. & MCNAUGHTON, P. A. (1989). Extrusion of calcium from rod outer segments is driven by both sodium and potassium gradients. *Nature* **337**, 740–743.

COREY, D. P. & STEVENS, C. F. (1983). Science and technology of patch-recording. In *Single Channel Recording*, ed. SAKMANN, B. & NEHER, E., pp. 53–68. Plenum Press, New York.

FENWICK, E. H., MARTY, A. & NEHER, E. (1982). A patch clamp study of bovine chromaffin cells and their sensitivity to acetylcholine. *Journal of Physiology* **331**, 577–597.

FRIEDEL, U. G., WOLBRING, G., WOHLFAHRT, P. & COOK, N. J. (1991). The sodium–calcium exchanger of bovine rod photoreceptors: K^+-dependence of the purified and reconstituted protein. *Biochimica et Biophysica Acta* **1061**, 247–252.

HILGEMANN, D. W. (1989). Numerical probes of sodium–calcium exchange. In *Sodium–Calcium Exchange*, ed. ALLEN, T. J. A., NOBLE, D. & REUTER, H., pp. 126–152. Oxford University Press, Oxford.

HODGKIN, A. L., MCNAUGHTON, P. A. & NUNN, B. J. (1985). The ionic selectivity and calcium dependence of the light-sensitive pathway in toad rods. *Journal of Physiology* **358**, 447–468.

HODGKIN, A. L., MCNAUGHTON, P. A. & NUNN, B. J. (1987). Measurement of sodium–calcium exchange in salamander rods. *Journal of Physiology* **391**, 347–370.

HODGKIN, A. L., MCNAUGHTON, P. A., NUNN, B. J. & YAU, K.-W. (1984). The effect of ions on retinal rods from *Bufo marinus*. *Journal of Physiology* **350**, 649–680.

HODGKIN, A. L. & NUNN, B. J. (1987). The effect of ions on sodium–calcium exchange in salamander rods. *Journal of Physiology* **391**, 371–398.

LAGNADO, L., CERVETTO, L. & MCNAUGHTON, P. A. (1988). Ion transport by the Na–Ca exchange in isolated rod outer segments. *Proceedings of the National Academy of Sciences of the USA* **85**, 4548–4552.

LAGNADO, L., CERVETTO, L. & MCNAUGHTON, P. A. (1992). Calcium homeostasis in the outer segments of retinal rods from the tiger salamander. *Journal of Physiology* **455**, 111–142.

LAGNADO, L. & MCNAUGHTON, P. A. (1991). Net charge transport during sodium-dependent calcium extrusion in isolated salamander rod outer segments. *Journal of General Physiology* **98**, 479–495.

LAMB, T. D., MCNAUGHTON, P. A. & YAU, K.-W. (1981). Spatial spread of activation and background desensitization in toad rod outer segments. *Journal of Physiology* **319**, 463–496.

LESER, G. P., NICOLL, D. A. & APPLEBURY, M. L. (1991). Distinctive properties of the purified Na–Ca exchanger from rod outer segments. *Annals of the New York Academy of Sciences* **639**, 222–233.

MCNAUGHTON, P. A., CERVETTO, L. & NUNN, B. J. (1986). Measurement of the intracellular free calcium concentration in salamander rods. *Nature* **322**, 261–263.

PERRY, R. J. & MCNAUGHTON, P. A. (1991). Characteristics of Ca_o and K_o binding sites of the Na–Ca, K exchange in isolated salamander rod outer segments. *Journal of Physiology* **434**, 70*P*.

SATHER, W. A. & DETWILER, P. B. (1987). Intracellular biochemical manipulation of phototransduction in detached rod outer segments. *Proceedings of the National Academy of Sciences of the USA* **84**, 9290–9294.

SCHNETKAMP, P. P. M., BASU, D. K. & SZERENCSEI, R. T. (1989). Na^+–Ca^{2+} exchange in bovine rod outer segments requires and transports K^+. *American Journal of Physiology* **257**, C153–157.

SCHNETKAMP, P. P. M. & SZERENCSEI, R. T. (1991). Effect of potassium ions and membrane potential on the Na–Ca–K exchanger in isolated intact bovine rod outer segments. *Journal of Biological Chemistry* **266**, 189–197.

SCHNETKAMP, P. P. M., SZERENCSEI, R. T. & BASU, D. K. (1991). Unidirectional fluxes through the bovine rod outer segment Na–Ca–K exchanger. *Journal of Biological Chemistry* **266**, 198–206.

YAU, K.-W. & NAKATANI, K. (1984). Electrogenic Na–Ca exchange in retinal rod outer segment. *Nature* **311**, 661–663.